AWARD NUMBER: W81XWH-21-1-0857

TITLE: An Innovative Approach for Noninvasive Evaluation of Stability at the Implant-Bone Interface for Transfemoral Osseointegrated Implants

PRINCIPAL INVESTIGATOR: Jacqueline Hebert

CONTRACTING ORGANIZATION: University of Alberta, Edmonton, Alberta, Canada

REPORT DATE: October 2022

TYPE OF REPORT: Annual

PREPARED FOR: U.S. Army Medical Research and Development Command
Fort Detrick, Maryland 21702-5012

REPORT DOCUMENTATION PAGE

Form Approved
OMB No. 0704-0188

1. REPORT DATE	2. REPORT TYPE	3. DATES COVERED
October 2022	Annual	15Sep2021-14Sep2022

4. TITLE AND SUBTITLE

An Innovative Approach for Noninvasive Evaluation of Stability at the Implant-Bone Interface for Transfemoral Osseointegrated Implants

5a. CONTRACT NUMBER
W81XWH-21-1-0857

5b. GRANT NUMBER
OR200058

5c. PROGRAM ELEMENT NUMBER

6. AUTHOR(S)

Jacqueline Hebert, Lindsey Westover, Mostafa Mohammed, Eric Beaudry

E-Mail: jhebert@ualberta.ca

5d. PROJECT NUMBER

5e. TASK NUMBER

5f. WORK UNIT NUMBER

7. PERFORMING ORGANIZATION NAME(S) AND ADDRESS(ES)

The Governors of the
University of Alberta
116 ST & 85 AVE
Edmonton, Alberta
T6G 2R3, Canada

8. PERFORMING ORGANIZATION REPORT NUMBER

9. SPONSORING / MONITORING AGENCY NAME(S) AND ADDRESS(ES)

U.S. Army Medical Research and Development Command
Fort Detrick, Maryland 21702-5012

10. SPONSOR/MONITOR'S ACRONYM(S)

11. SPONSOR/MONITOR'S REPORT NUMBER(S)

12. DISTRIBUTION / AVAILABILITY STATEMENT

Approved for Public Release; Distribution Unlimited

13. SUPPLEMENTARY NOTES

14. ABSTRACT. The objective is to develop a non-invasive evaluation tool to assess the stability of osseointegrated implants. We have built physical models of implants integrated in bone surrogates to conduct benchtop experiments. We investigated the response of the implant system to various excitation parameters. Incorporating the implant components that are used in the clinical setting has guided the parameters that we have investigated for the redesign such as the excitation direction (transverse vs. axial), impact mass, and impact rod tip. We have developed and validated a novel analytical modeling approach specific to the implant system. We have developed finite element models of the system to allow simulations in both the modal analysis and explicit time domain to better understand the response to impact loading and to cross-validate with the experimental data analysis. Through our testing and modelling, we have learned that the acceleration measurement on the impact rod alone does not provide sufficient data and as such, we have developed and validated a new approach to monitor the acceleration on the implant system. This important step, as well as development of new electronics, communication, and software interfaces has allowed us to collect both laboratory and clinical participant data using the existing version of the impact hand piece while we work towards a redesigned hand piece.

15. SUBJECT TERMS Osseointegration, transfemoral amputation, bone-implant stability, dynamic response, vibration response, finite element modelling

16. SECURITY CLASSIFICATION OF:			17. LIMITATION OF ABSTRACT	18. NUMBER OF PAGES	19a. NAME OF RESPONSIBLE PERSON
a. REPORT	b. ABSTRACT	c. THIS PAGE			USAMRDC
Unclassified	Unclassified	Unclassified	Unclassified	33	19b. TELEPHONE NUMBER *(include area code)*

TABLE OF CONTENTS

1. **INTRODUCTION:**

This project addresses the focus area: *Osseointegration - Identification of best practices to address failure of percutaneous osseointegrated prosthetic limbs.* We are developing and validating a non-invasive clinical evaluation tool to assess the stability of osseointegrated implants through the measurement of the stiffness of the bone-implant interface. The tool will be based on our Advanced System for Implant Stability Testing (ASIST) device, which was developed for assessment of percutaneous bone conduction hearing aid implants. The objective of our research is to adapt the ASIST technique for bone-anchored hearing aids for use with larger transfemoral OI implants through the development of a redesigned mechanical handpiece and analytical model, and prospective *in vivo* evaluation of longitudinal changes in patients receiving a transfemoral OI implant. We hypothesize that the developed ASIST technique will provide a reliable and objective measure of stability at the implant-bone interface. This technique could then be deployed to test the ability to show preceding (early changes) before detected failure, and to document rates of bone-implant integration, thereby providing a method to track bone-implant integration and detect early loosening.

2. **KEYWORDS:**

Osseointegration, transfemoral amputation, bone-implant stability, dynamic response, vibration response, finite element modelling

3. **ACCOMPLISHMENTS:**

- **What were the major goals of the project?**

The major goals of the project are to (1) redesign and manufacture the ASIST device to optimize the vibration response in relation to the size of the implant; (2) develop a new analytical model for the implant and cross-validate using finite element analysis, and (3) collect prospective observational data in a cohort of 10 patients undergoing transfemoral OI to validate the experimental model and to provide preliminary data on the rate of change and range of ASC values over the expected time of healing and osseointegration.

- **SOW Tasks**. Status indicated below. Tasks for year 2-4 labelled N/A.

Specific Aims 1&2: (1) Optimize the vibration response of the ASIST device in relation to the size of the implant; (2) Develop and cross-validate the analytical model		
Major Task 1: Redesign the ASIST device	**Months**	**STATUS**
Subtask 1: Design and manufacture mechanical handpiece, electronics and communications	1-6	In progress
Subtask 2: Program preliminary software and user interface	3-9	Complete
Subtask 3: Build physical models, conduct experimental bench tests for validation	6-12	80% complete
Subtask 4: Ongoing device evaluation and technical support, manufacture additional units for testing	12-24	N/A
Milestone(s) Achieved - Prototype ASIST device complete and validated for collecting acceleration data	12	45% achieved
Major Task 2: Develop and validate the analytical model		
Subtask 1: Develop analytical model	6-12	Complete

Subtask 2: Develop finite element model	6-12	Complete
Subtask 3: Validate models with benchtop experimental data	6-24	In progress
Milestone(s) Achieved: Validated analytical model for ASC values	24	60% achieved
Specific Aim 3: Collect prospective observational data in a cohort of 10 patients undergoing transfemoral OI to validate and define ASC value ranges		
Major Task 1: Conduct observational study	**Months**	**STATUS**
Subtask 1: Prepare regulatory documents and research protocol for observational study	1-6	Completed
Subtask 2: Submit ethics to IRB and HRPO secondary review	3-6	Completed
Subtask 3: Submit NACTRC operational approvals	3-6	Completed
Milestone(s) Achieved: HRPO approval for all protocols, local IRB approval, NACTRC operational approvals	9	Completed
Major Task 2: Participant Recruitment and data collection		
Subtask 1: Screen, consent and enroll 10 participants	9-30	20% achieved
Subtask 2: Schedule for data collection sessions	12-42	In progress
Subtask 3: Collect ASIST data	12-42	In progress
Subtask 4: Collect and interpret radiographic (Xray) images	12-42	N/A
Subtask 5: Extract data from clinical outcomes trial	36-42	N/A
Milestone(s) Achieved: Data collected and collated for 10 participants	42	
Major Task 3: Data analysis and translation		
Subtask 1: Validation of ASIST using participant experimental data against model	25-45	N/A
Subtask 2: Data analysis and interpretation of participants ASC values	37-45	N/A
Subtask 3: Compile results for dissemination	45-48	N/A
Subtask 5: Transition ASIST software for commercialization	25-36	N/A
Subtask 4: Investigate and finalize transition and commercialization pathway	25-48	N/A
Subtask 5: Regulatory meetings for next phase	38-48	N/A
Milestone(s) Achieved: Completed documentation for ASIST validation and translation plan	48	

- **What was accomplished under these goals?**

Summary of accomplishments:

In the first year of the project, we have made significant progress in **Major Task 1** (Redesign the ASIST device) and **Major Task 2** (Develop and validate the analytical model). We have built several physical models of implants integrated in bone surrogates (Sawbones) to conduct experimental tests for benchtop validation of the approach. We have developed preliminary versions of the electronics, communication, and software interfaces to enable data collection in both the laboratory and clinical environments. Through our benchtop testing (Major Task 1) and modelling (Major Task 2), we have learned that the acceleration measurement on the impact rod alone does not provide sufficient data for analysis and as such, we have developed and validated an approach to monitor the acceleration on the implant system as well. This important step has allowed us to collect both benchtop and clinical data using the existing version of the impact hand piece while we work towards a redesigned hand piece.

We have made significant progress on understanding the implant system and its response to excitation through our benchtop experimental testing and our modelling efforts. Understanding the implant components that are specifically used in the clinical setting, such as the bushings and connectors, has guided the parameters that we have investigated for the hand piece redesign such as the excitation direction (transverse vs. axial), impact mass, and impact rod tip design. The extensive benchtop work from Year 1 has provided valuable information for the development stage of the new hand piece, which will progress in the upcoming year with the hiring of a new engineer focused on the hand piece redesign and device development.

Year 1 goals for Major Task 2 is substantially complete. We have developed and validated a novel analytical modeling approach specific to the transfemoral implant system. We have developed finite element models of the system to allow simulations in both the modal analysis and explicit time domain to better understand the implant system and its response to impact loading, to cross-validate and better understand the experimental (benchtop) data analysis, and to guide the new hand piece development. As per the statement of work (Major Task 2: Subtask 3), the benchtop data validation will continue through Year 2 of the project.

Detailed description of activities:

Specific Aim 1: Optimize the vibration response of the ASIST device in relation to the size of the implant

1. Major Task 1: Redesign the ASIST Device

1.1 Subtask 1: Design and manufacture mechanical handpiece, electronics and communications

1.1.1. Prototype actuation

A magnetically actuated electro-mechanical handpiece was first rapidly prototyped from T-slot aluminum bar, two sizes of bear-quality 316 stainless steel (medical grade), two sizes of high-load dry-running sleeve bearings, three sizes of electromagnet, five sizes of neodymium magnet, and various 3D-printed supports. The T-slot architecture allowed us to adjust the prototype into numerous configurations and provided a sturdy base that minimized the amount of variability in strike positions when striking the implant. Two sizes of 316 stainless steel bar were selected to test the effect of mass on vibration response of the implant. A 5 mm diameter rod was cut to 75 mm in length to obtain a mass of 11.75 g; an 8 mm diameter rod was cut to 100 mm in length to obtain a mass of 40.16 g. The dry-running bearings were selected in accordance with the rod diameters and provided adequate performance throughout testing. Preliminary testing with magnetic actuation from small, bored solenoids was relatively unsuccessful. It was immediately apparent that the impact rods would not be able to attain the velocities required for significant implant excitation with these solenoids.

It was thus hypothesized that larger electromagnets with ferromagnetic cores could provide sufficient actuation. Three sizes of stock electromagnet were selected: 5, 15, and 25 kg holding force.

Five 1/8'' neodymium magnets were selected for fixation to the rear of the impact rod: 1/16'', 1/8'', 3/16'', 1/4'', and 1/2'' length. The electromagnets were energized by an oscillating DC current, which repelled or attracted the permanent neodymium magnets fixed to the back of the impact rods. This repulsion and attraction would cause the impact rod to extend, striking the implant, and then retract. Both impact rods were threaded at the striking end and assembled with a matching nut. This provided a limit on the linear motion of the impact rods. Power was provided to the electromagnets by a variable current or voltage DC power source. The voltage applied to the electromagnets was frequently manipulated to elicit different magnetic flux densities. An Arduino board with a mounted motor shield was used for electromagnet control. The primary Arduino code was developed to energize the electromagnets 16 times in 4 s (4 Hz), which matched the striking frequency of the Periotest. The code also allowed for different 'extension times', the length of time that a voltage was applied to the electromagnets. A schematic of the prototype is shown in **Figure 1.**

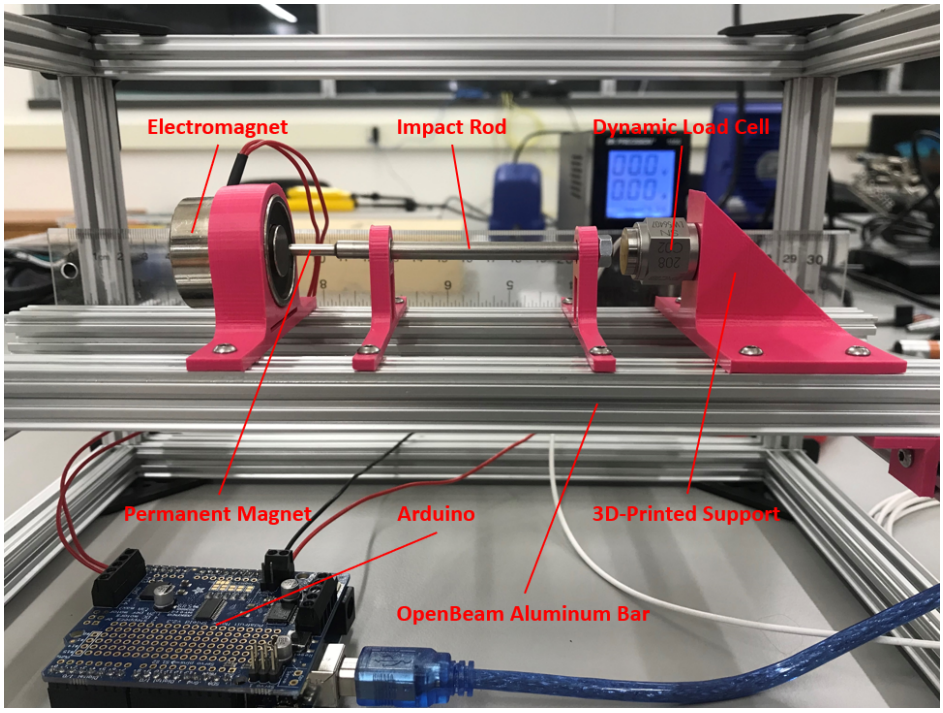

Figure 1: First iteration prototype with impact load cell

Testing was conducted to discern a feasible prototype configuration for further testing and optimization. Velocity testing was initially conducted with both impact rods. In this test, an iPhone with a high-speed frame rate camera recorded the extension of the impact rods with different combinations of neodymium magnets and electromagnets. The hypothesized strongest electromagnet (25 kg holding force) was tested with all available neodymium magnets, and the hypothesized strongest neodymium magnet (1/2'' length) was tested with all available electromagnets. The electromagnets were energized by a 5 VDC source. This voltage was chosen because it was the rated voltage for all the electromagnets. It was found that only the 15 kg holding force electromagnet in combination with the 1/2'' length neodymium magnet on the 5 mm diameter impact rod could match the velocity specified for the Periotest in the literature (0.17 m/s). This result indicated that we would need the strongest electromagnet and neodymium magnet combination possible to effectively actuated the impact rod. The experiment velocity chart can be viewed in **Figure 2**. Surprisingly, the 15 kg holding force electromagnet outperformed the 25 kg holding force electromagnet with respect to velocity. Upon measurement with a Gauss meter, it was confirmed that at the same applied voltage, the 15 kg holding force electromagnet could also generate a greater magnetic flux density than the other two electromagnets (Fig 3). However, the magnetic flux density of all magnets could be linearly increased by raising the applied voltage. The electromagnet magnetic flux densities can be viewed in **Figure 3**.

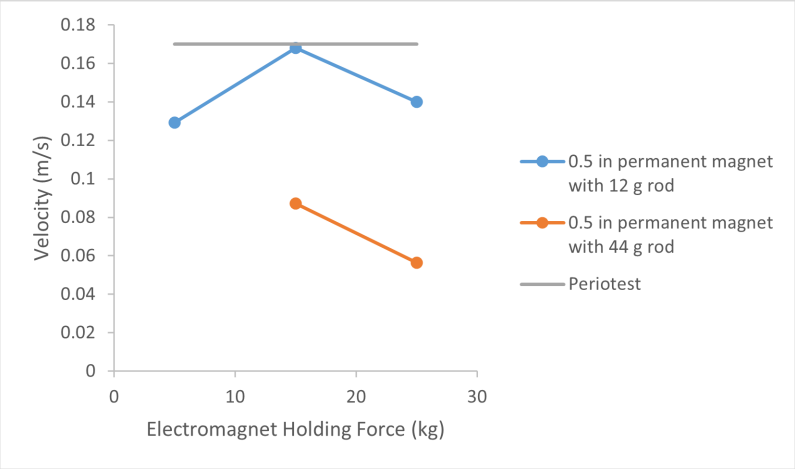

Figure 2: Impact rod average velocity vs. electromagnet holding force.

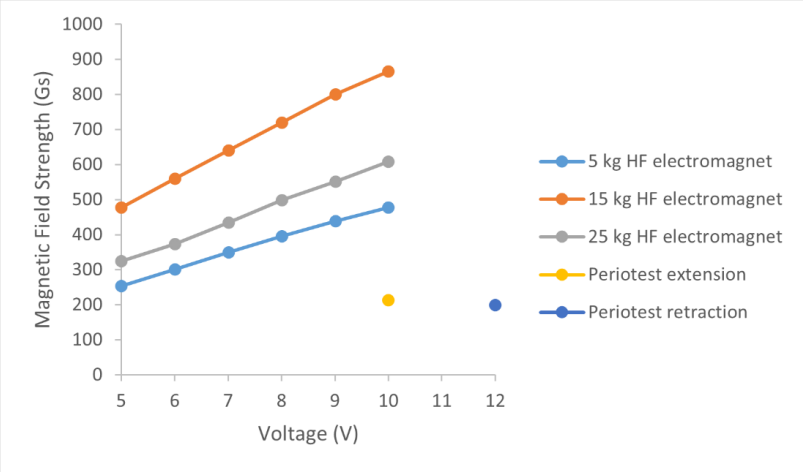

Figure 3: Magnetic flux density vs. voltage applied to electromagnet

In the next set of performance tests, a PCB impact load cell (pictured in Figure 1) was implemented. Although only one prototype configuration had matched the velocity of the Periotest, it was thought that the greater masses of the prototype impact rods compared to the Periotest impact rod could yield greater impact forces overall. Additionally, we knew that raising the voltage applied to the electromagnets could increase impact velocities and forces. The load cell was directly mounted to the T-slot bar structure and struck head-on by the impact rods. The 15 kg holding force electromagnet was tested with all neodymium magnets, and the 1/2'' length neodymium magnet was test with all electromagnets. Three voltages (5, 7.5, and 10 V) and three extension times (50, 75, and 100 ms) were tested. It was found that different prototype configurations could match or exceed the impact forces generated by the Periotest in the same experimental setup. It was noted that, in general, under the same excitation conditions, the larger rod could generate greater impact forces. However, the larger rod was also more difficult to consistently excite due to the presence of large static friction forces. The 5 mm diameter impact rod in combination with the 15 kg holding electromagnet and 1/2'' length neodymium was deemed to be the setup with the most potential. It could generate impact forces matching or exceeding the Periotest and could be consistently excited at a wide range of voltages and extension times. Further testing was done with the setup to generate characterization curves (pictured in **Figure 4**). The bottom of the curves enter the domain of the Periotest impact force (40 N), while the high end of the curves reach up to 90 N. This wide range is an exciting achievement, as higher impact forces may be necessary to optimally excite the bone-implant system.

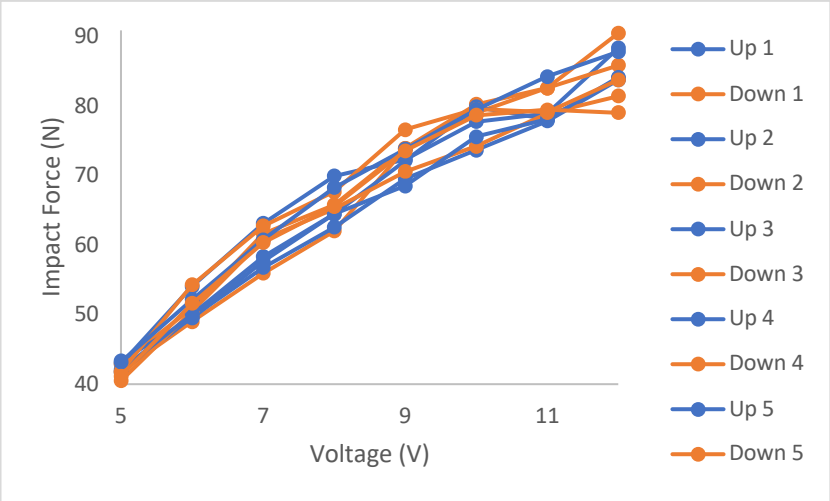

Figure 4: Impact force vs. voltage applied to 15 kg holding force electromagnet

1.1.2 Investigating parameters for impact force

One of the key challenges of developing the handpiece has been finding a configuration that can optimally excite the larger bone-implant system. Specifically, it is desirable to excite as many modes of vibration as possible for a given bone-implant interface condition. We hypothesized that transferring more energy to the system could cause more modes to be excited. We investigated several ways achieve this goal. In the simplest approach, we conducted tests where impact force was manipulated by altering the voltage or extension time applied to the 15 kg holding force electromagnet. We recorded the acceleration response of the implant through an accelerometer mounted on the dual cone adapter of the implant with double-sided tape. We used the prototype setup (5 mm diameter impact rod; 1/2'' length neodymium magnet; 15 kg holding force electromagnet) to strike the dual cone adapter in the transverse position. We found that increasing the striking force by increasing the voltage applied to the electromagnet only served to increase the amplitude of the implant acceleration signal. There were otherwise no signal-to-signal characteristic differences.

Another approach to improve implant excitation was to alter the 'contact time' of the impact event, by altering the length of time that the impact rod was in contact with the implant during collision. We explored this possibility by fixing five different materials to the head of the impact rod. In order of ascending Young's modulus, the materials were: neoprene rubber, silicone rubber, Delrin (plastic), aluminum, and steel (impact rod material). After striking the impact load cell with each material, we found that the lower modulus materials lowered peak impact force and prolonged contact time (see **Figures 5 and 6**). After transversely striking the implant and recording the acceleration signals, it became apparent that the lower modulus materials (neoprene, silicone, and Delrin) only served to damp out desirable high frequency components of the signals. Aluminum and steel performed similarly in all cases and were both able to excite at least two modes of vibration (see **Figures 7 and 8**). Therefore, 316 stainless steel was selected as the tip material for its durability, pre-existing use as the impact rod body material, and sufficient transverse excitation of the bone-implant system (superglue interface; dual cone adapter attachment). Impact force will be further fine-tuned in the upcoming stages of handpiece development.

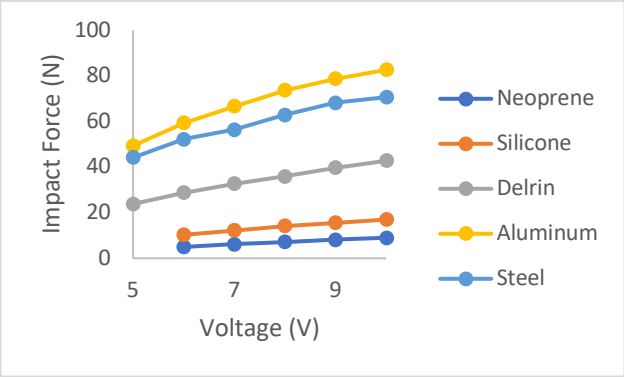

Figure 5: Impact force vs. voltage applied to 15 kg holding force electromagnet

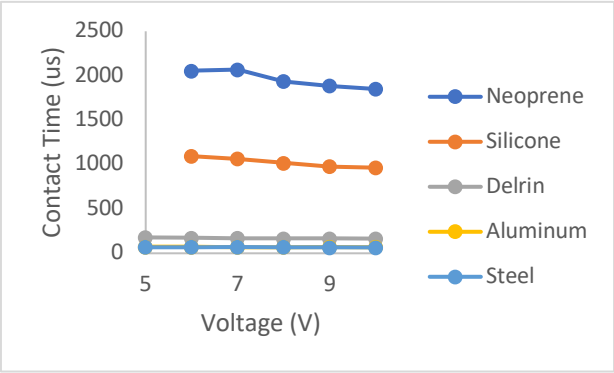

Figure 6: Contact time vs. voltage applied to 15 kg holding force electromagnet

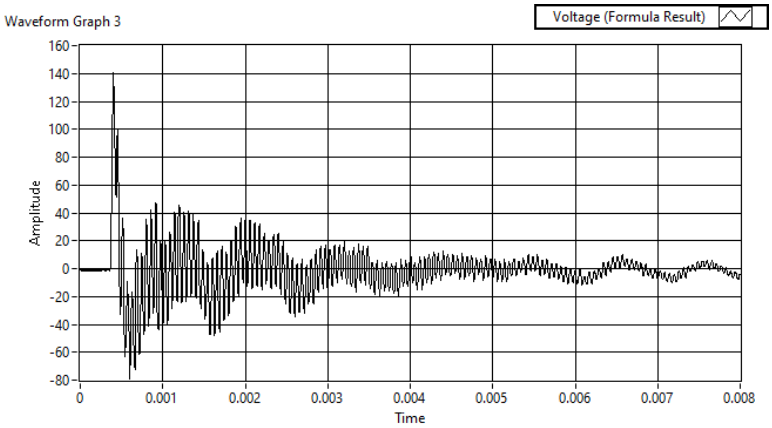

Figure 7: Time domain acceleration response of strike with 10 g rod, aluminum interface, and 7 V applied to electromagnet

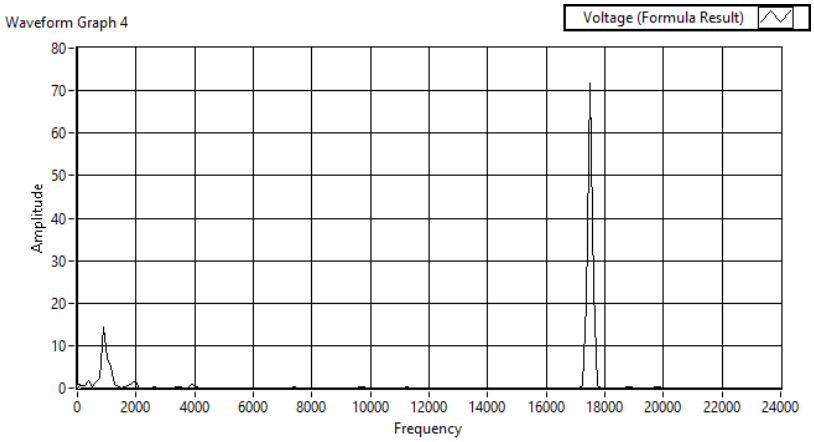

Figure 8: Frequency domain acceleration response of strike with 10 g rod, aluminum interface, and 7 V applied to electromagnet

1.1.3 Investigating excitation requirements of the clinical system

The introduction of the GV connector to the bone-implant system, which attaches onto the dual cone adapter, posed new problems for implant excitation and acceleration signal acquisition. Initially, the acceleration signals collected for transverse implant excitation with the GV connector contained much more noise than the signals without the GV connector. We also noticed an interesting phenomenon in the prior series of experiments and a set of intermediate repeatability tests. We noticed that even minute differences in strike alignment (angle between the implant surface and axis of the impact rod) could influence the characteristics of the acceleration signal. Testing with only the dual cone adapter revealed that what when the flat surface of the impact rod impacted the implant in such a way that the surfaces were mated together, higher frequency modes could be excited. If the surfaces did not mate perfectly upon impact or the strike was not 'flush', lower frequency modes would dominate the signal. This information was applied in the next series of experiments.

To rapidly come up with a solution to obtain a more harmonic and less noisy signal with the GV connector installed on the implant, a multiple factor experiment was devised. We tested the effects of mass, strike orientation, strike interface geometry, and presence of the GV connector on the acceleration response of the bone-implant system with superglue interface. The striking mass was either a pendulum (10, 20, 50, 100, or 200 g) or one of the two original impact rods with a mass secured mid-rod via double-sided tape (10, 20, 30, 40, 50, 60, 70, or 90 g total). The latter prototype setup was added to control variability in the experiment after initial testing with the pendulum setup. The pendulum was only used for transverse dual cone strikes without the GV connector. The strike orientations were either transverse or axial. The strike interface geometry was manipulated by either striking with the flat or pointed surface of the pendulum. The striking setup can be viewed in **Figure 9.**

Results indicated that noise was most limited for striking masses between 10 and 60 g across all setups. For setups with the GV connector, axial strike orientations presented more harmonic and less noisy acceleration signals than transverse strike orientations. In general, it appeared that pendulum strikes with the flat surface excited greater contributions from high frequency modes than pendulum strikes with the pointed surface. The harmonic and repeatable nature of acceleration responses from axial strikes, even with the GV connector on, was a particularly exciting outcome from this set of experiments. The experiments did, however, have a handful of drawbacks. While a subset of striking masses that limited signal noise were discovered, the exact effect of altering the striking mass could not be discerned. The pendulum strikes were highly uncontrolled, and although improvements were made using the impact rods, there was still some degree of uncertainty associated with the nonuniform distribution of mass on the impact rods. Moreover, the exact effect of strike interface geometry remained largely uninvestigated in a controlled way.

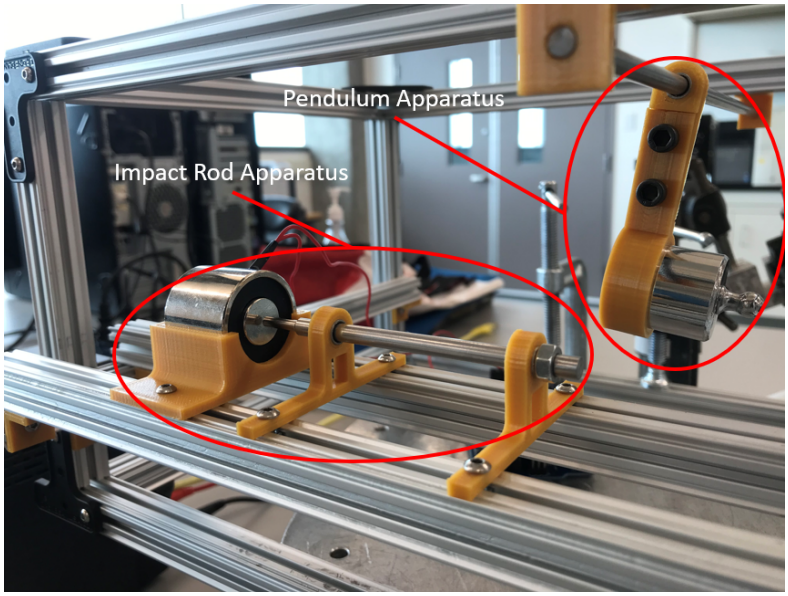

Figure 9: Impact rod and pendulum apparatus

1.1.4 Next experiment set up

With certainty that mass and tip/strike interface geometry are important factors in mode excitation, noise reduction, and repeatability, a final experiment (data acquisition ongoing) was designed to optimize the prototype device configuration. The factors in this experiment include seven custom machined impact rods of six different masses, three different tip geometries, strike orientation, bone-implant interface adhesive, strike orientation, and presence of the GV connector. 10, 20, and 30 g impact rods were machined from 5 mm diameter 316 stainless steel. 30, 40, 50, and 60 g impact rods were machined from 8 mm diameter 316 stainless steel. Two different diameter rods were implemented to ensure reasonable impact rod lengths. There is overlap between the different diameter rods at one mass (30 g) to discern if diameter has any effect on acceleration response. The tip geometries are machined flat, conic, and hemispherical threaded caps. The strike orientations are axial or transverse. The bone-implant interface adhesives are silicone or superglue.

Higher mass impact rods are hypothesized to consistently excite more modes of vibration across different configurations, while potentially introducing greater noise to the system. Conic and hemispherical tip geometries are hypothesized to improve signal repeatability (small variations in strike angle have less of an effect), while the flat geometry is hypothesized to be able to excite high frequency modes of vibration in transverse orientations without the GV connector. Axial signals are hypothesized to be more harmonic and have less noise than transverse signals for configurations with the GV connector. Data collection has commenced for the silicone setup configurations (setup in **Figure 10**).

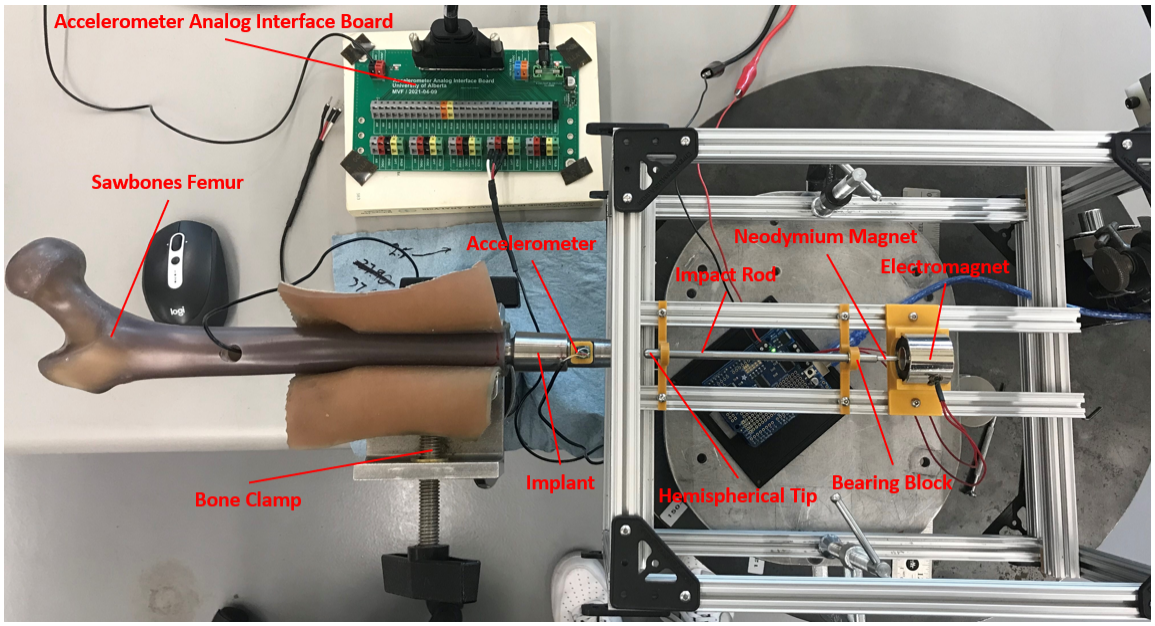

Figure 10: Prototype validation test experimental setup. The OI implant is installed in the sawbone with silicone interface. The impact rod with electromagnet actuation provides controlled stike forces for the benchtop experiments.

1.2 Subtask 2: Program preliminary software and user interface

Refer to description under Specific Aim 3, Major Task 2 (2.3 Subtask 3: Collect ASIST data on participants, page 21). Briefly, measurements have been collected using a miniature data acquisition setup developed inhouse using a TEENSY 4.1 microcontroller (PJRC) to have the same acquisition capabilities (acquisition rate) as the national instruments systems used in the lab. The software and user interface development has improved the clinical portability of the data collection system and standardized the lab-based benchtop experiments (detailed in 2.3 Subtask 3, page 17).

1.3 Subtask 3: Build physical models, conduct experimental bench tests for validation

Physical models have been constructed from synthetic bones (Sawbones); implants, dual cone adapters, and GV connectors; adhesives such as silicone and superglue to replicate different interface conditions; and bone clamps or vices. As described under Section 1.1 (Subtask 1) above, validation tests have been initiated for various prototype configurations. See Figure 10 for the current physical model setup (silicone interface) for ongoing experiments under this Aim. Note that physical models have been shared and developed in conjunction with the works under Major Task 2, Subtask 3. See Section 2.3.1 for detailed description of physical models and experimental bench tests.

Major Task 1 - Milestone (Month 12) - Prototype ASIST device complete and validated for collecting acceleration data.

Since its inception, the prototype has gone through several iterations and continues to be optimized for use with transfemoral implants. The prototype has an effective magnetic actuation system and can be configured to exactly replicate Periotest performance. This performance continues to be altered and optimized to transfemoral implants. The prototype can excite and collect accelerations signals from a transfemoral implant 16 times in 4 s. Acceleration signals can be collected through either a robust data acquisition system or a clinic friendly Teensy board. LabVIEW software has been developed to collect and average acceleration signals as well as extract frequency spectra. The prototype system is capable of simultaneously exciting and detecting multiple modes of vibration for certain bone-implant interface conditions. We have developed preliminary versions of the electronics, communication, and software interfaces to enable data collection in both the laboratory and clinical environments, thereby allowing us to collect both benchtop and clinical data using the existing version of the impact hand piece while we work towards a redesigned hand piece. Ongoing experimental validation works described under Subtask 1 will lead to a robust device that is optimized to collect measurements from transfemoral implants.

Specific Aim 2: Develop and cross-validate the analytical model

2, Major Task 2: Develop and validate the analytical model

2.1 Subtask 1: Develop analytical model

2.1.1 Major Activities of Subtask 1:

Initially, the system was modelled using discrete analytical models where the system components (such as the stem and the dual cone adapter) where represented as rigid bodies connected to each other and to the bone using spring elements (**Figure 11**). Under this analytical representation the system had a limited number of degree of freedoms (DOF) and was unable to capture some of the vibrating modes of interest such as the complex bending behavior shown below (**Figure 11**). Increasing the number of DOFs along the system did not significantly improve the accuracy of the analytical model. Therefore, the system was represented using a simplified 1D finite element (FE) model based on Timoshenko beam theory on MATLAB® (Mathworks). The 1D FE code has demonstrated superior mathematical power of representing the dynamic response of the bone-implant system and preserved the computationally efficiency of the code which makes it ideal within a clinical setting. The 1D FE representation was cross validated with the 3D ABAQUS® model using both: (1) Frequency and (2) time domain analysis and has demonstrated significant potential.

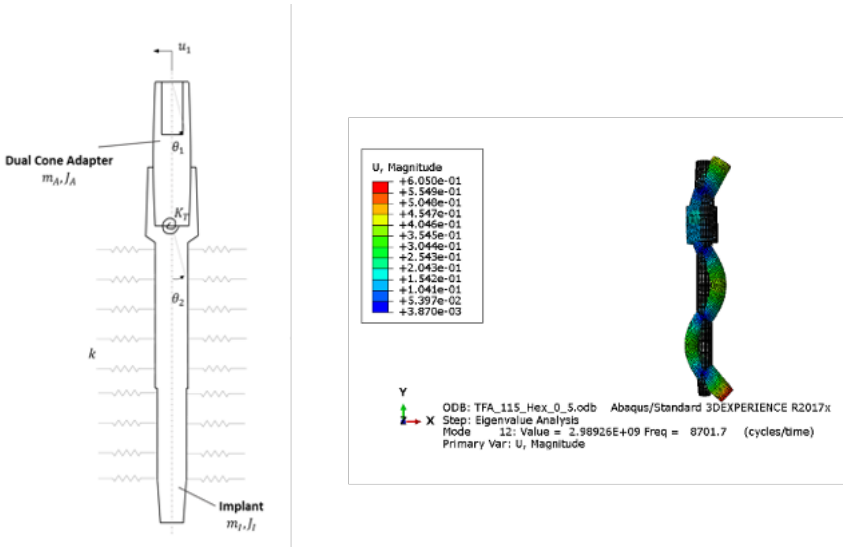

Figure 11. Old analytical representation of the system (Left): The system was represented by two rigid bodies (the dual cone adapter (m_A, J_A) and the implant (m_I, J_I)) with limited set of DOFs (u_1, θ_1, θ_2) and spring elements (K_T, k). This analytical representation could not capture some complex bending modes such as this bending behavior (Right).

2.1.2 Significant Outcomes of Subtask 1:

The dynamic response of the system using the 1D FE code was analyzed in the: (1) Frequency domain (Modal analysis) and in (2) the time domain. The former is meant to check the model's power in approximating the natural frequencies and mode shapes while the latter checks the model's power in evaluating the response under the actual loading condition (for example the response of the system under impact).

The complete methodology and results of the frequency (Modal) analysis were published in the Canadian Society of Mechanical Engineers Proceedings [1]. In Summary, the 1D FE model: (1) was validated with well-established theories, (2) captured all the vibration modes of interest accurately for two extreme interface conditions (**Figure 12** and **Figure 13**) and (3) showed that k (interface stiffness) has the potential to be a stability metric that is independent of the implant geometry. Similarly, the 1D FE model time domain response was cross validated with the 3D ABAQUS® (Dassault Systèmes) model to predict the dynamic behavior of the system under the actual loading conditions. The results of the time domain analysis are reported in the next section under 2.2 subtask 2.

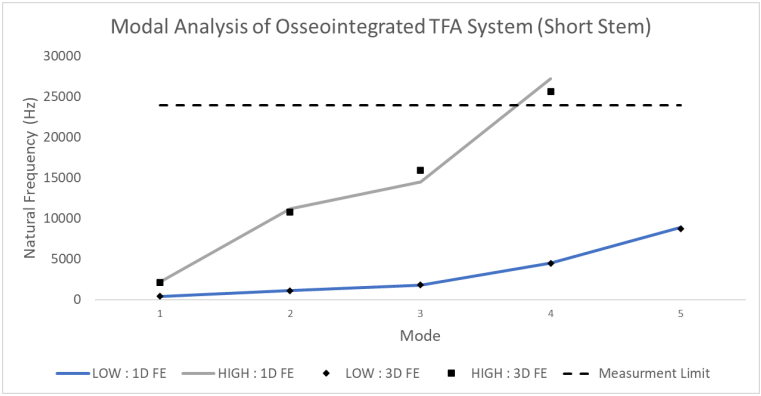

Figure 12. Natural Frequency prediction using the 1D FE model and the 3D ABAQUS® model for two extreme interface conditions of an actual bone-implant system.[1]

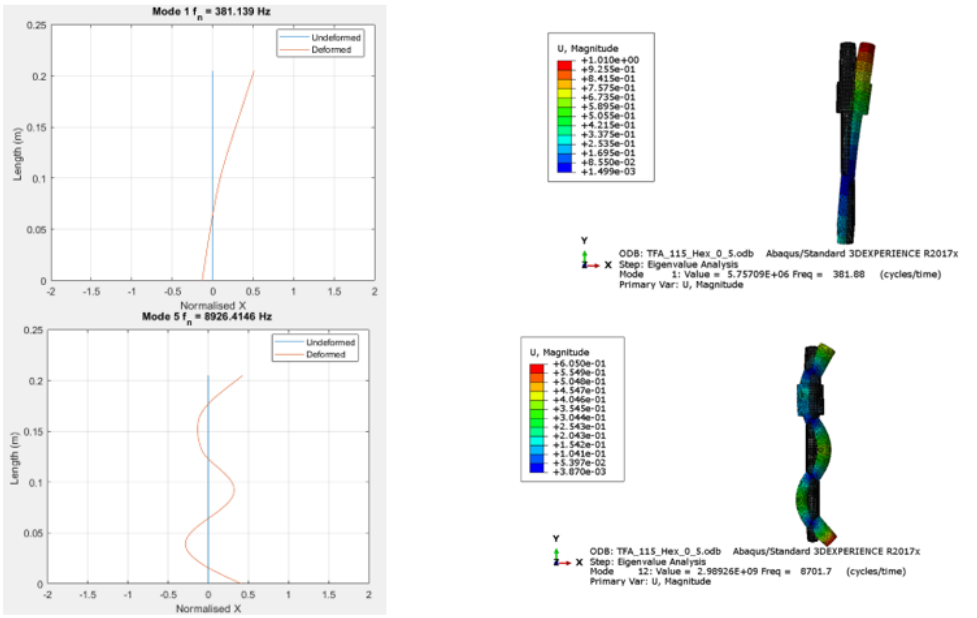

Figure 13. The 1D FE code (Left) was able to capture all of the bending modes of interest accurately compared to the 3D ABAQUS® model (Right).[1]

2.2 Subtask 2: Develop finite element model

2.2.1 Major Activities of Subtask 2:

A finite element model of the bone implant system is constructed on ABAQUS®. A schematic of the model is shown in **Figure 14.** Similar to the analytical model, the model is composed of the dual cone adapter and the transfemoral stem. However, unlike the 1D FE code the 3D ABAQUS® model has the capacity to estimate the out of plane effects experienced by the system instead of the strictly planar behavior of the 1D FE model. Additionally, the bone and the bone implant interface are modelled accurately using well defined geometries and mechanical properties compared to their simplified representation using linear springs. Therefore, it can be deduced that the finite element representation is more capable of representing the physical system. The model can be used to perform two main types of analysis: (1) Dynamic (time integration) analysis and (2) Frequency (Eigenvalue) analysis. The former can be used to assess the time domain response of the system (**Figure 14**) under a specific loading condition (for e.g., impact generated by the rod) while the latter assess the generalized response (frequency and mode shapes) of the system under no particular loading scenario.

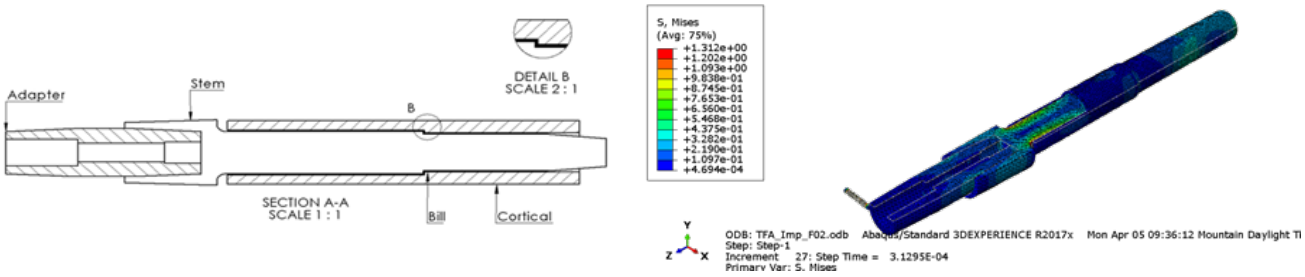

Figure 14. Schematic of the bone implant system's components used for constructing the finite element model (Left). The response of the system (Von Mises Stress field) upon impact generated by the time integration (explicit) finite element model (Right).

2.2.2 Significant outcomes of Subtask 2:

The 3D ABAQUS® model offers a better representation of the actual physical bone-implant system yet isolates the response from potential noise encountered during in-vitro and clinical acquisitions. Thus, it provides a baseline for cross validating the 1D FE model. As it was outlined in the previous section, the 3D ABAQUS® model has been used in cross validating the modal response of the 1D FE model. In addition to this, the time domain response under impact loading was evaluated and compared to the 1D code (Error! Reference source not found.). Although there is a relatively high Pearson Correlation Coefficient (similarity) between the 1D and 3D models in terms of the displacement response, the acceleration response (which is related to the displacement by a multiplicative factor of the natural frequencies squared) is more prone to magnifying any difference in the natural frequencies between the 1D and 3D FE models. Therefore, the 1D and 3D FE codes are similar, however evaluating the response using a time domain metric may not be the best possible avenue for comparing the signals. Transforming the response to the frequency domain shows that the signals coming from the 1D and 3D FE models are similar in terms of the peaks alignment (**Figure 16**) and further cements that the 1D FE code is working properly.

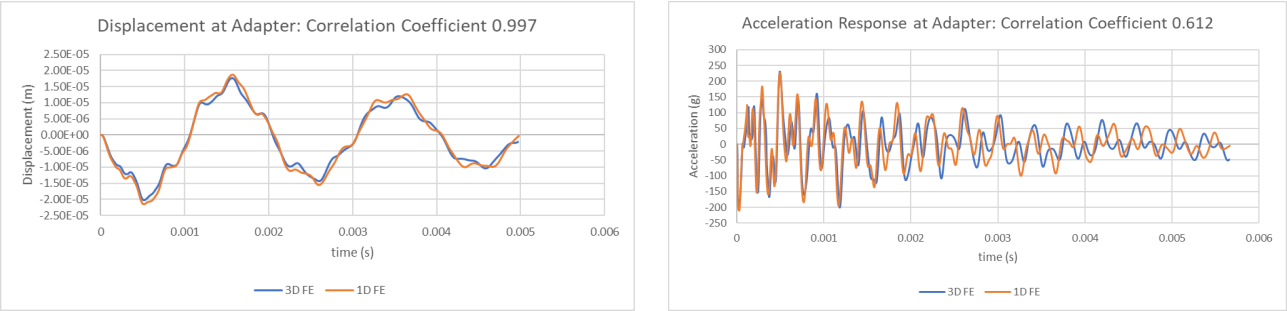

Figure 15. Time domain displacement of the 1D and 3D FE models shows that the 1D code is able to capture response with high similarity (left). The acceleration response has a lower similarity coefficient due to the magnification of the errors (Right).

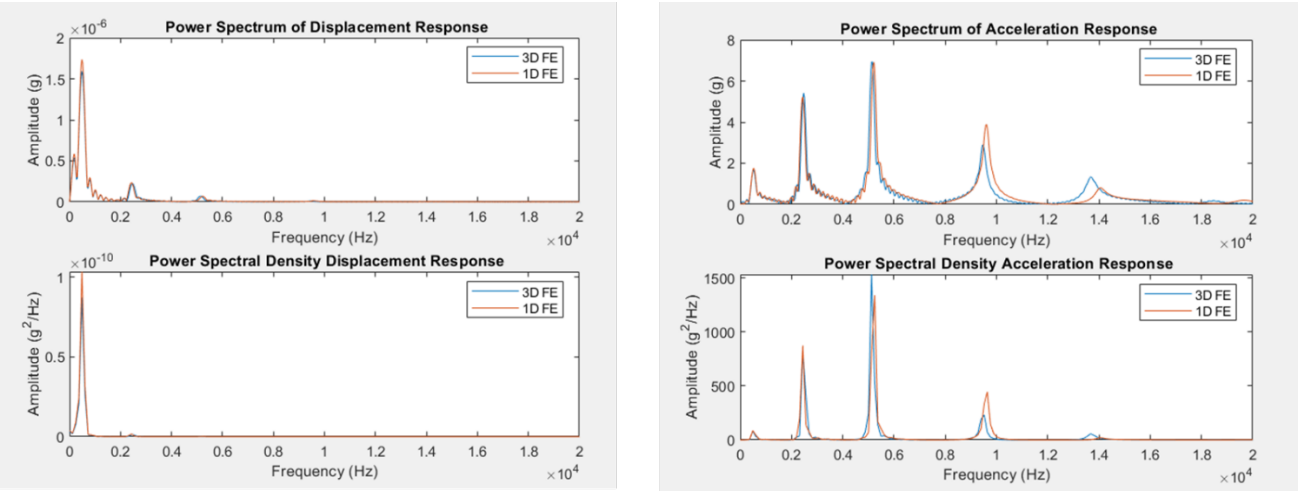

Figure 16. Converting the time domain response to the frequency domain shows that the both the displacement (Left) and acceleration (Right) signals are matching and that the higher differences in the acceleration are due to magnifying the differences rather than dissimilarity between the models.

2.3 Subtask 3: Validate models with benchtop experimental data

2.3.1 Major Activities Subtask 3:

2.3.1.1. Simplified Benchtop Setup.

As a starting point a simplified in-vitro representation of the bone implant system was developed (**Figure 17**) using a straight cylinder (SAWBONES 3403-36) that has the same material properties of the cortical shaft. The setup consists of a 140 mm stem and 68.5 mm dual cone adapter that are assembled using the internal locking screw which is tightened to 10 Nm to mimic the in-vivo torque level. The femoral canal was drilled to be larger than the stem at the interface region by 0.2 mm, this gap allowed for the application of a superglue interface region between the stem and the bone. Acceleration measurements were taken using ADXL 1004 (Analog Devices©) accelerometer mounted on the dual cone adapter. The simplified setup was used to assess the main parameters that affect the acceleration response to help with designing the detailed experiment outlined in section 2.3.1.2. Additionally, it was used to pre-assess the ability of the mathematical (FE) models in representing the bone implant system.

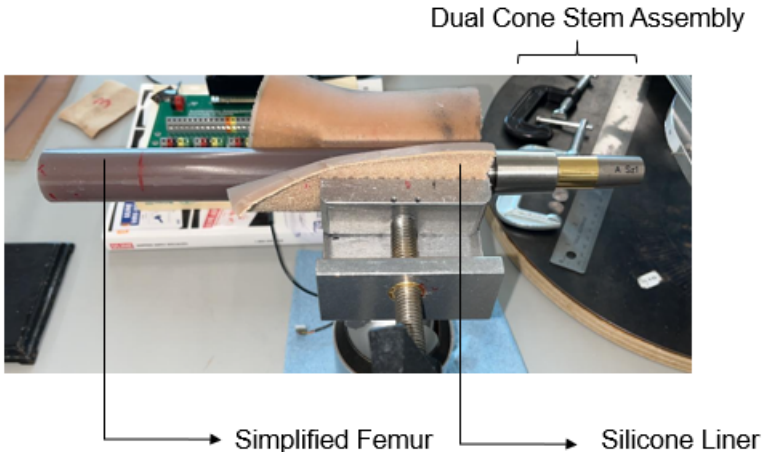

Figure 17. Simplified bone-implant system representation.

The frequency response obtained from the simplified experimental setup under transverse and axial loads is shown in **Figure 18**. The bending response is dominated by one frequency at 1160 Hz while the axial response is dominated by a single frequency at 10750 Hz. Those values are in range with the 3D FE modal analysis values of 1220 Hz and 11733 Hz for transverse and axial modes respectively.

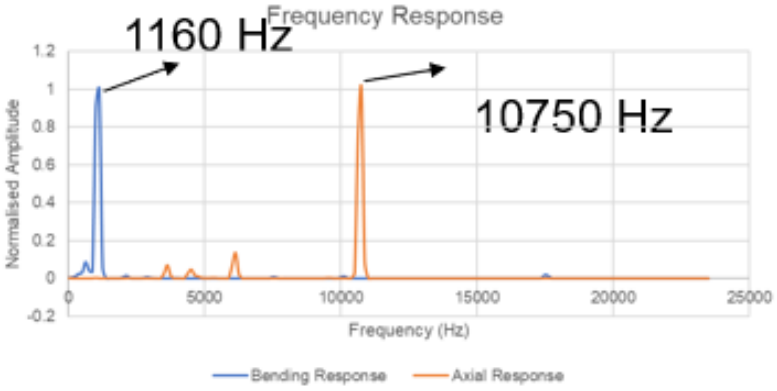

Figure 18. The bending and axial response obtained from the in-vitro simplified setup.

2.3.1.2. More representative Benchtop Setup:

The simplified benchtop experiment was used to identify the important variables that should be investigated using the more representative in-vitro setup of the bone implant system **(Figure 19**). Table 1 summarises the main variables investigated in this experiment. The first variable, the interface material, is used to assess the sensitivity of the acceleration response (measurement) to the interface condition. Silicone rubbers have low stiffness and can represent a situation with negligible tensile stiffness like fibrous tissue formation while superglue has a considerably higher stiffness and can model healing healthy bone. The second variable investigates adapter length, to determine the effect of the system's geometry on the response and the effectiveness of the model to isolate the geometric effects on evaluating the interface condition. Thirdly, accelerometer mounting techniques can affect its performance and therefore two different techniques are used to assess the quality of the measurement. Finally, different loading and boundary conditions are applied to see the effectiveness of the excitation mechanism and the effect of different femoral boundary conditions on the measurements. This is a balanced 2^5 design with 5 repetitions, where each repetitions involves reinstalling the bone implant system into the femoral clamp (re-applying the boundary and excitation conditions). Changing the interface condition and extracting the implant stem from the bone involves breaking the bone and therefore all the measurements must be sequentially collected for both interface conditions. To date, the measurements for all the silicone interface conditions have been collected and we are in the process of finalising the measurements for the superglue interface setup.

Figure 19. More representative bone-implant experiment.

Table 1. Balanced 2^5 design Matrix of the main variables and their levels for the more representative in-vitro setup.

Variable	Level 1 (LOW)	Level 2 (HIGH)
Interface	Silicone Rubber	Superglue
Adapter Length	68.5	108.5
Mounting	Double Sided Tape	Superglue
Loading	Transverse	Axial
Bone Boundary Condition	Fully Fixed with Liner	Cantilever

2.3.1.3 Preliminary findings of the more representative bone implant model:

This section presents some of the preliminary findings of the ongoing experiment. Table 2 shows a comparison between the FE models and the recorded frequencies from the experiment for the silicone setup. The experimental data was collected using two accelerometers; an external accelerometer placed at the adapter and an internal accelerometer placed on the stem's tip (near the femoral head). The first observation from the findings is that both accelerometers agree on their readings, which indicates that the detected vibrations are potential modes of vibration rather than noise. Additionally, the detected modes seem to be close to the 1D and 3D model predictions for both transverse and axial excitation which indicated that the model is one step closer to validation and that there is more reliability in its predictions. **Figure 20** shows the difference in the experimental transverse response of the LOW and HIGH stiffness interface situations, as it can be observed the dominant peak (which is the 2nd transverse mode from the model) experienced an increase of around 60% in the measurement and this indicates that this mode is sensitive to the interface condition under the current conditions. **Figure 21** shows that the change in the axial response for the two interface conditions, as it can be observed the dominant mode experienced an increase in the dominant frequency, however this increase is relatively modest (3%) compared to what was observed in the transverse mode. From the FE models, it seems that the Periotest (current impactor) is only exciting the 2nd axial mode for the LOW interface situation and is unable to excite the 1st axial mode while for the HIGH interface situation it is exciting the 1st axial mode. To establish a more objective comparison, finding means to excite the 1st axial mode for the LOW stiffness situation will allow us to better evaluate the sensitivity of the axial mode to the interface condition. This can potentially be achieved by using a larger impactor: **Figure 22** shows the effect of increasing the mass of the impactor to 40 g, which is able to increase the contribution of the 1st axial mode in the signal.

Table 2. Comparison between the model and the experiment for the LOW (silicone) Interface situation

Pre-liminary analysis of LOW Interface results: Comparison between Experiment and the Model			
Mode	Model (Hz)	Experiment (Hz) (External Accelerometer)	Experiment (Hz) (Internal Accelerometer)
Transverse Mode 1	262	250	250
Transverse Mode 2	590	583	583
Transverse Mode 3	1703	Not Observed	Not Observed
Transverse Mode 4	2746	2500	2500
Axial Mode 1	665	Not Observed	Not Observed
Axial Mode 2	9385	9333	Accelerometer was in transverse orientation

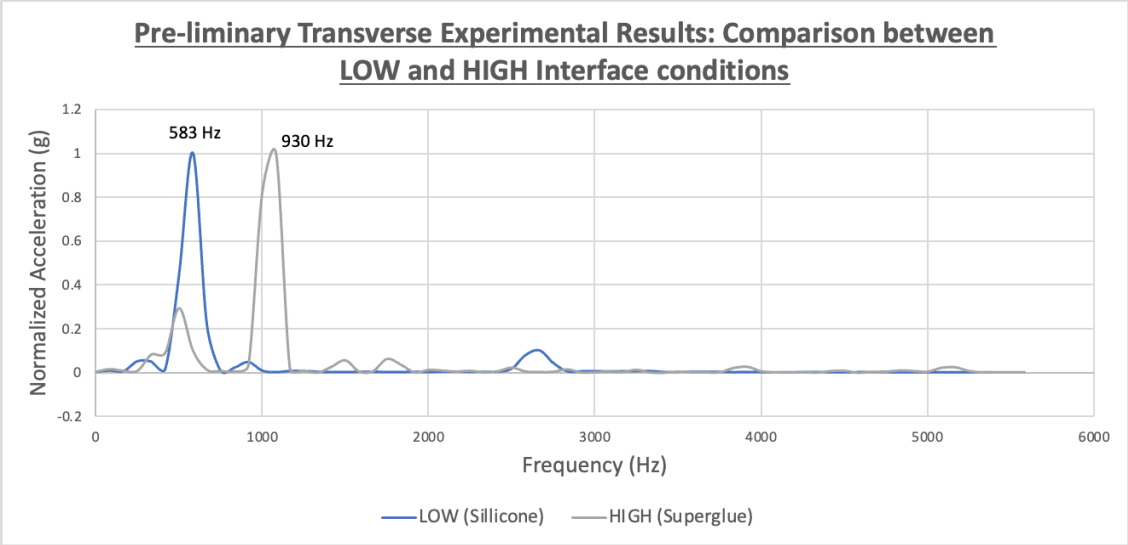

Figure 20. Comparison between the dominant transverse frequency for different interface conditions.

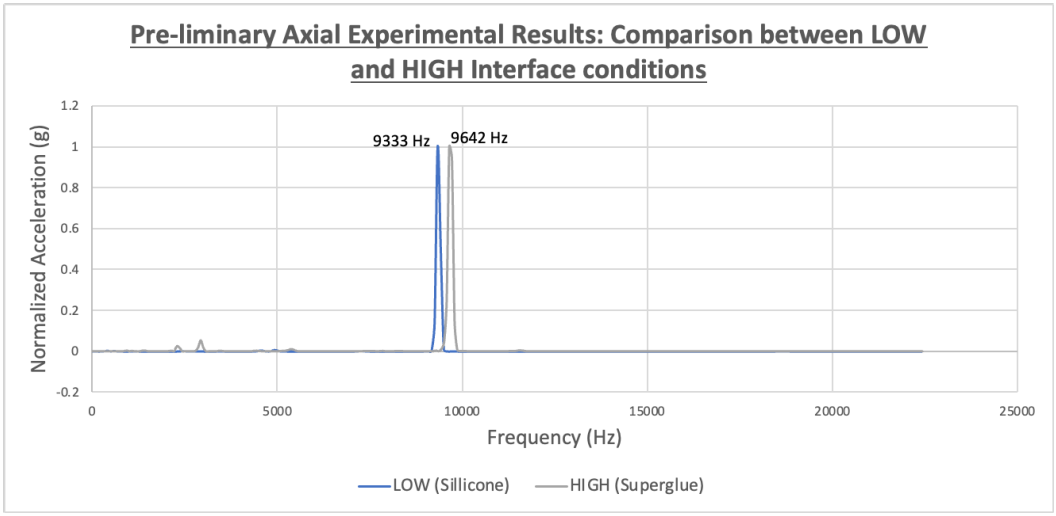

Figure 21. Comparison between the dominant axial frequency for different interface conditions.

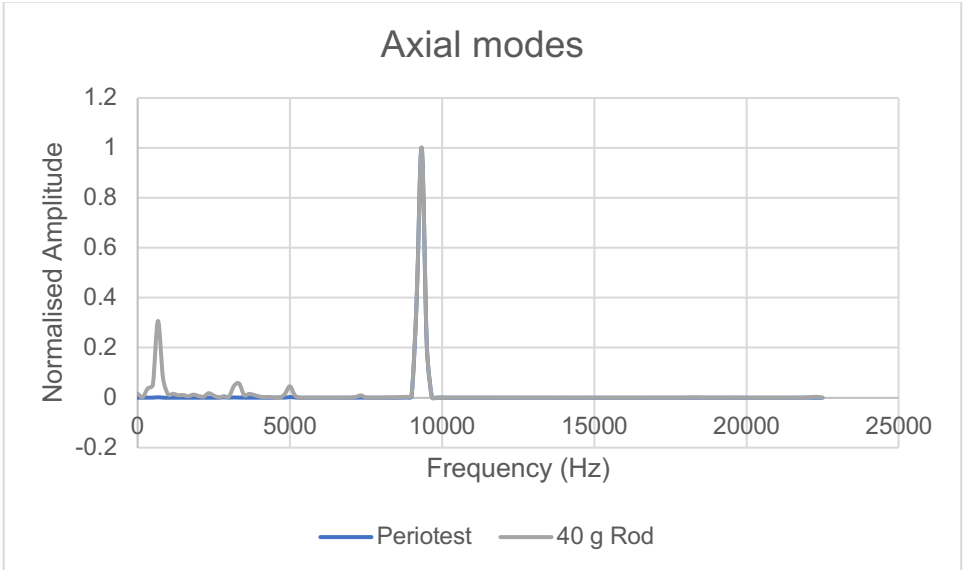

Figure 22. Potential of Increasing the sensitivity of the axial modes by using a larger impactor for the LOW interface situation.

2.4 Summary of Specific Aim 2 and next steps

The 1D and 3D FE mathematical models seem to agree in both frequency and time domain analysis. This agreement indicates that the mathematical premise for the 1D model is valid and has potential to be used as a representation of the bone implant system for clinical assessment of the interface situations. Furthermore, the ongoing experiments have further indicated the use of these mathematical models since there is agreement between the models (1D and 3D) models' prediction and the experiment. Preliminary, analysis of the response detected between the silicone (LOW) and superglue (HIGH) interface conditions indicate that our measurement is sensitive to the interface condition in the transverse mode and has potential to be very sensitive under the axial condition if there are more efficient means of exciting the 1st axial mode.

Next steps involve finalizing the remaining experimental measurements and analysing the collected experimental results. The analysis will then allow us to distinguish between the important variables that require further analysis and the less significant ones that can be dismissed. Therefore, the next step would involve continued benchtop experimentation and comparisons with the model to study its capabilities and its limitations in measuring implant stability and the interface condition.

Specific Aim 3: Collect prospective observational data in a cohort of 10 patients undergoing transfemoral OI to validate and define ASC value ranges

1. Major Task 1 – All subtasks completed.

Milestone achieved: HRPO approval for all protocols, local IRB approval, NACTRC operational approvals.

2. Major Task 2 – Participant recruitment and data collection. In progress.

2.1 Subtask 1. We have screened, consented, and enrolled 2 participants. This is on target to anticipated quarterly enrollment goals.

2.2 Subtask 2. Schedule for data collection. We have conducted 9 measurements sessions for the first participant and 7 measurement sessions for the second participant.

2.3 Subtask 3: Collect ASIST data.

The measurements were collected using a miniature data acquisition setup developed inhouse using a TEENSY 4.1 microcontroller (PJRC) to have the same acquisition capabilities (acquisition rate) as the national instruments systems used in the lab (**Figure 23**). The instruments used in the clinic can record all the 14 strikes we initiate using the Periotest as shown in **Figure 24** without losing data. Moreover, for a given testing session the strike repeatability is high (**Figure 25**). To analyse the collected data, the analysis code has to consider applying some digital filtering and windowing functions to reduce undesirable noise features such as spectral leakage. **Figure 26** shows a raw frequency spectrum, as it can be observed the dominant frequencies are hard to observe, however when a windowing function is applied the peaks become distinguishable and the obtained results become more similar to the data collected experimentally and predicted with the model. We are currently in the process of selecting the most appropriate signal processing functions to apply on the clinically acquired samples to analyse them without losing important features of the signal characteristics.

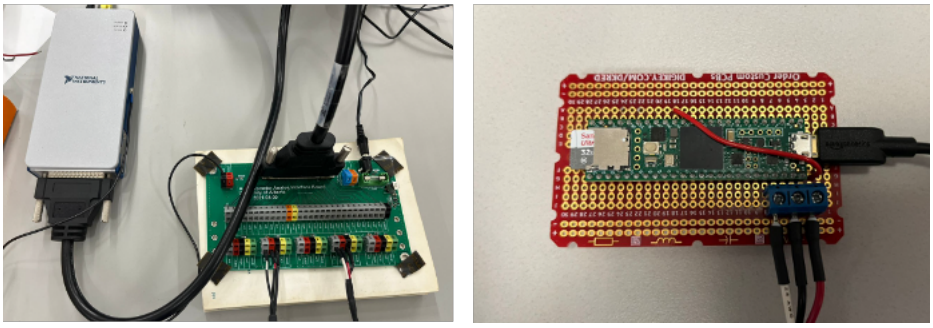

Figure 23. The National Instruments data acquisition system used for the benchtop experiments (Left) and the clinical acquisition setup developed in house using a Teensy 4.1 board (Right).

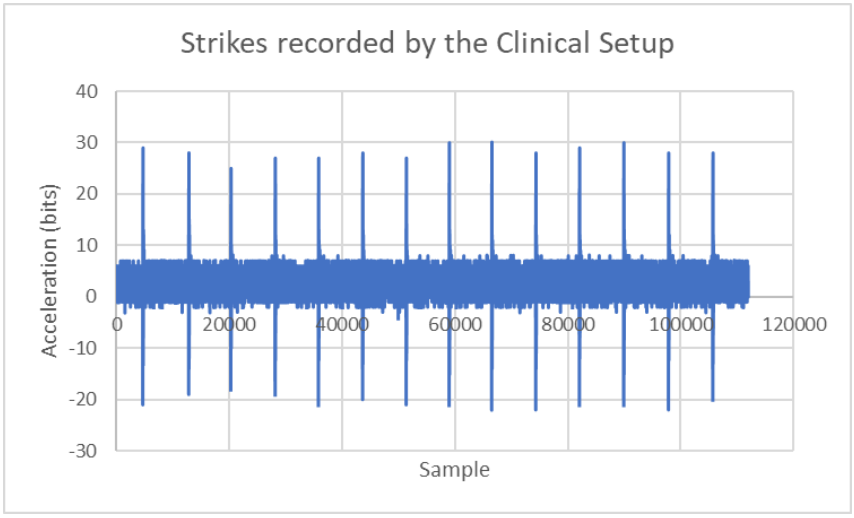

Figure 24. A selected clinical sample recorded by the clinical DAQ. The Periotest (current impactor) generates 16 strikes per test and the clinical data acquisition (developed inhouse using Teensey 4.1) is able to consistently record the 14 strikes. The 1st and 16th strikes are used for triggering the DAQ.

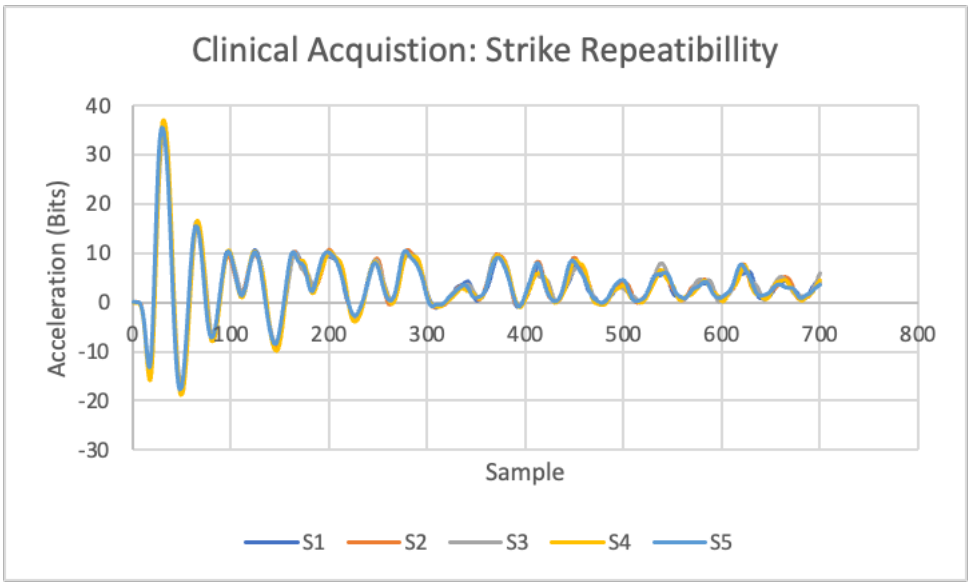

Figure 25. The figure shows randomly selected strikes from one of the clinical testing sessions. The figure shows that the strikes generated by the Periotest and recorded by the DAQ have high repeatability potential.

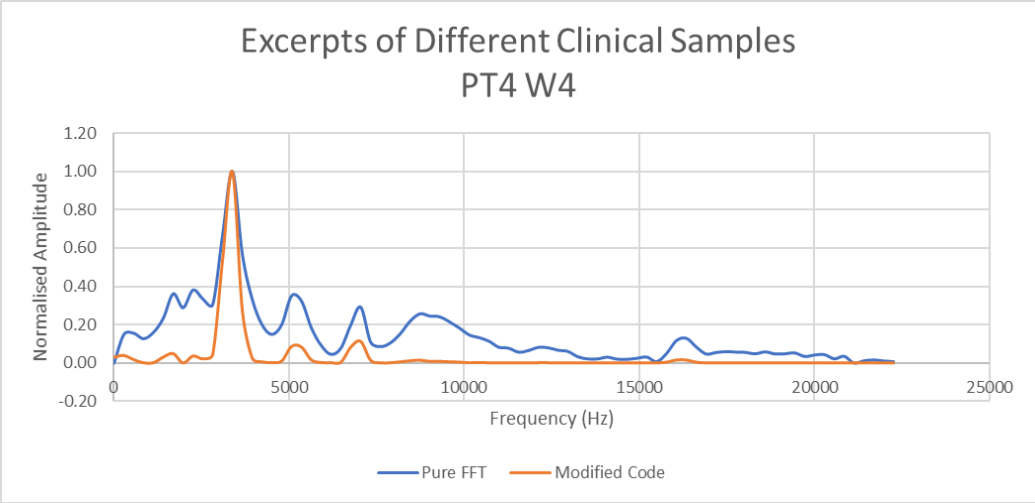

Figure 26. Effect of applying a windowing function to reduce spectral leakage and improve the analysis.

- **What opportunities for training and professional development has the project provided?**

Nothing to report

- **How were the results disseminated to communities of interest?**

Nothing to report

- **What do you plan to do during the next reporting period to accomplish the goals?**

Specific Aim 1 & 2

Major Task 1: Redesign ASIST device. We will complete the experiments detailed in 1.1.4. investigating the parameters: impact rod mass, tip geometry, strike orientation, interface condition, GV connector. Based on these experimental results, we will finalize the design requirements for the prototype device.

Major Task 2: Develop and Validate analytical model. The next steps involve finalizing the remaining experimental measurements and analysing the collected experimental results. The analysis will allow us to distinguish between the important variables that require further analysis and the less significant ones that can be dismissed. Therefore, the next step involves continued benchtop experimentation and comparisons with the model to study its capabilities and its limitations in measuring implant stability and the interface condition.

Specific Aim 3, Major task 2: Additional participant recruitment and ongoing data collection from clinical participants.

4. **IMPACT:**

- **What was the impact on the development of the principal discipline(s) of the project?**

Nothing to report.

- **What was the impact on other disciplines?**

Nothing to report.

- **What was the impact on technology transfer?**

Nothing to report.

- **What was the impact on society beyond science and technology?**

Nothing to report.

5. **CHANGES/PROBLEMS:**

- **Changes in approach and reasons for change**

Nothing to report

- **Actual or anticipated problems or delays and actions or plans to resolve them**

We have had a delay in hiring a full-time engineer on the project. We have now identified a hire and are awaiting the work permit application to be approved, with anticipated start date January 2023. We mitigated the delay by assigning existing engineering personnel onto the project, but this has only been 50% of their time, therefore progress is a bit slower on the development side than anticipated. We therefore shifted the focus of our work to the experimental data collection and have made better than expected progress on defining and validating the analytical model and design criteria for the device. The handpiece redesign will be the major focus of the starting engineer.

- **Changes that had a significant impact on expenditures**

The delay in hiring the engineer has reduced our expenditures this year; we plan to carry over the funds to support the engineer for the next 3 years of the project.

- **Significant changes in use or care of human subjects, vertebrate animals, biohazards, and/or select agents**

  Not applicable.

- **Significant changes in use or care of human subjects**

  Not applicable.

- **Significant changes in use or care of vertebrate animals.**

  Not applicable.

- **Significant changes in use of biohazards and/or select agents**

  Not applicable.

6. **PRODUCTS:**

- **Publications, conference papers, and presentations**

  - **Journal publications.**

    Nothing to report.

  - **Books or other non-periodical, one-time publications.**

    Nothing to report.

  - **Other publications, conference papers, and presentations.**

    - Conference Proceedings:

    Mohamed M, Raboud D, Hebert JS, Westover L. Stability Assessment of Osseointegrated Transfemoral Bone-Implant Systems using Finite Element Modal Analysis. In: Progress in Proceedings of the Canadian Society for Mechanical Engineering International Congress 2022. Edmonton; 2022.

- **Website(s) or other Internet site(s)**
  Not applicable.

- **Technologies or techniques**
  Not applicable.

- **Inventions, patent applications, and/or licenses**
  Not applicable.

- **Other Products**
  Not applicable.

7. **PARTICIPANTS & OTHER COLLABORATING ORGANIZATIONS**

- **What individuals have worked on the project?**

Name:	Jacqueline Hebert
Project Role:	*PD*
Researcher Identifier (e.g. ORCID ID):	*0000-0003-0788-0568*
Nearest person month worked:	*1.2*
Contribution to Project:	*Project director / lead PI; has coordinated and supervised the team efforts on the project to date, including overall project management, clinical testing, and reporting requirements.*
Funding Support:	*University of Alberta salary*

Name:	Lindsey Westover
Project Role:	*PI*
Researcher Identifier (e.g. ORCID ID):	*0000-0003-1220-3967*
Nearest person month worked:	*1.2*
Contribution to Project:	*Co-Principle investigator, led the engineering efforts in the redesign of the handpiece and ASIST modelling, and is the main supervisor of the graduate students on the project*
Funding Support:	*University of Alberta salary*

Name:	Mostafa Mohamed
Project Role:	*Graduate student*
Researcher Identifier (e.g. ORCID ID):	*0000-0001-5082-4823*
Nearest person month worked:	*12*
Contribution to Project:	*Mr. Mohamed has performed the work in the area of model analysis (analytical and finite element models) and the experimental data collection with clinical participants.*
Funding Support:	

Name:	*Eric Beaudry*
Project Role:	*Graduate Student*
Researcher Identifier (e.g. ORCID ID):	
Nearest person month worked:	*12*
Contribution to Project:	*Mr. Beaudry has conducted the benchtop experiments for the design of the mechanical handpiece.*
Funding Support:	

Name:	*Ahmed Shehata*
Project Role:	*Research Associate*
Researcher Identifier (e.g. ORCID ID):	*0000-0001-8442-9901*
Nearest person month worked:	*6*

Contribution to Project:	*Dr. Shehata has overseen the engineering research and development efforts and experimentation, including assisting and advising the graduate students.*
Funding Support:	

- **Has there been a change in the active other support of the PD/PI(s) or senior/key personnel since the last reporting period?**

  Nothing to report

- **What other organizations were involved as partners?**

  Nothing to report

8. **SPECIAL REPORTING REQUIREMENTS**

   - **COLLABORATIVE AWARDS:** N/A
   - **QUAD CHARTS:** updated and submitted with attachments.

9. **APPENDICES:**

Proceedings of the Canadian Society for Mechanical Engineering International Congress 2022
CSME Congress 2022
June 5-8, 2022, Edmonton, AB, Canada

Stabillity Assessment of Osseointegrated Transfemoral Bone-Implant Systems using Finite Element Modal Analysis

Mostafa Mohamed[1*], Don Raboud[2], Jacqueline S Hebert[3], Lindsey Westover[4]
[1]Mechanical Engineering, University of Alberta, Edmonton AB, Canada
[2] Mechanical Engineering, University of Alberta, Edmonton AB, Canada
[3] Division of Physical Medicine and Rehabilitation, University of Alberta, Edmonton AB, Canada
[4] Mechanical Engineering, University of Alberta, Edmonton AB, Canada
*mostafa5@ualberta.ca

Abstract

The dynamic response of osseointegrated implant systems can be used to evaluate the condition of the bone-implant interface (BII) and implant stability. The primary objective of this work is to develop a simplified dynamic 1D finite element (FE) model of the OPL transfemoral amputation (TFA) bone-implant system. The model's intended clinical use is to compare the collected acceleration response from an impact with the percutaneous adapter to the model's prediction and solve for the unknown BII stiffness. The model utilizes linear vibration theory and thus should accurately capture the natural frequencies and mode shapes of interest. A simply supported uniform beam was modelled using Euler-Bernoulli, Rayleigh, and Timoshenko FE beam formulations and compared with the analytical solution for validation. Additionally, a 3D ABAQUS® model was developed and it showed that Timoshenko's formulation is the most appropriate model due to the significant shearing effects of the higher modes. Afterwards, a simply supported TFA implant system was modelled with the 1D FE code and compared to the 3D ABAQUS® model. The results indicated that the 1D FE model accurately predicted the natural frequencies of interest with a maximum difference of 3.08 %. The interface stiffness was then introduced as a series of springs distributed over the effective length of the stem. The stiffness' magnitude was controlled by k which was the total stiffness normalized with respect to the volume of the stem's effective length. The matching between the 1D and 3D models was based on manipulating the k to match the first mode frequency and comparing the results for the remaining modes. This yielded highly similar natural frequencies and mode shapes for a short stem (effective length=115 (mm)) with two extreme interface conditions. The same values of k found for the short stem were then used to perform modal analysis for a long stem (effective length=160 (mm)) and it yielded highly similar results between the 1D and 3D models which indicates that k is independent from the implant's geometry. The numerical analysis performed in this investigation sets the groundwork for a series of additional in-vitro and in-vivo analysis of TFA systems and ultimately the development of a non-invasive vibration-based stability measurement system.

Keywords: Lower Limb Amputations; Finite Element Method; Implant Stabillity; Modal Analysis; Transfemoral Implants; Osseointegration

I. INTRODUCTION

Traditionally, patients with lower limb amputations undergo rehabilitation using socket prosthesis which can be associated with skin irritation, higher degrees of discomfort, frequent need for refitting, and improper sizing issues for a short residual stump [1]–[3]. Since the 1990s, osseointegrated transfemoral amputation (TFA) implant systems have been introduced as an alternative to socket prosthesis [1], [3]. To date, there are two TFA systems that have passed the clinical trial phase and are being used in various parts of the world: (1) the OPRA and (2) the OPL systems [1], [2]. The OPRA system achieves primary (mechanical) stability using a screw fixated intramedullary stem while OPL implants rely on press fitting the stem into the femoral canal [3]. Both implant systems achieve secondary stability through osseointegration in which osseous material is directly deposited on the stem's surface by bone growth and remodeling, leading to the formation of the bone-implant interface (BII) [3], [4].

Assessing osseointegrated implant stability is critical to determining the success of the surgery, early failure detection, and designing patient specific rehabilitation programs [4], [5]. Vibration based methods rely on analyzing the dynamic response of the bone-implant system and correlating implant stability to a system parameter such as the natural frequency [4], [5]. Such methods have demonstrated great potential for osseointegrated dental implants and hearing aids due to their non-invasive and quantitative nature [5]–[8]. As for TFA systems, in-vitro vibration analyses of the OPRA system have shown promise in detecting BII condition changes [9]–[11].

The primary limitation of relying on the natural frequency as an implant stability metric, is that the natural frequency is not solely dependent on the BII; it is also influenced by other

parameters such as the implant geometry and thus cannot be used as an absolute stability metric [12], [13]. Coupling the dynamic response of the implant system with a mathematical model can overcome this limitation and allows for the estimation of the BII condition directly [8], [13]. There are different approaches to mathematically modelling a dynamic bone-implant system. For example, simple systems can be modelled as rigid bodies connected with linear springs and analyzed using the discrete form of Newton's 2nd law [13]. Systems can also be modelled as continuous systems using partial differential equations (PDEs). Analytical solutions of PDEs exist however, major assumptions are required regarding the geometry and boundary conditions. The finite element (FE) method is a numerical approach for satisfying the weak form of the PDE in a weighted residual sense and can be used for problems with complex geometries and boundary conditions [14].

The primary goal of this investigation is to develop a mathematical model that can capture the dynamic behavior of the OPL implant system accurately yet is computationally efficient in assessing the BII condition in a clinical setting. Preliminary testing involved exciting the system using transverse impact loads and measuring the response at the percutaneous adapter using an ADXL 1004 accelerometer (Analog Devices), revealed that the acceleration response is dominated by several (five at most) bending modes. Therefore, it is required that the model captures the first five bending modes accurately or covers the measurement bandwidth of the accelerometer (24 KHz) for a wide range of BII conditions. It is hypothesized that constructing a 1D FE model of the bone-implant system using an appropriate beam formulation under dynamic loading will satisfy those requirements.

The objective of this work is to develop a 1D FE code that performs modal analysis of the bone-implant system and report its capabilities and limitations. The first step in this investigation involves validating the FE code by comparing it to the analytical solution of a simply supported uniform beam with the same length to diameter (*L/D*) of a TFA implant. Moreover, the results are compared to a 3D FE model constructed on ABAQUS® (Dassault Systèmes). Afterwards, the 1D FE code is compared to a 3D FE ABAQUS® model for an actual TFA implant geometry. Finally, the interface stiffness is introduced to the model and the eigenvalues and eigenmodes are compared between the 1D FE code and 3D FE model for two implant geometries (short and long) and two extreme interface conditions (fibrous and healthy bone). It should be noted that this study focuses on mathematically analyzing the dynamic behavior of the bone-implant system as an eigenvalue problem. It sets the foundation for further mathematical, in-vitro and in-vivo time domain analysis, since the time domain response is the linear superposition of several modes of vibration according to linear vibration theory [15].

II. METHODS

A. Mathematical basis for the 1D FE Code.

A beam is a planar structure subjected to transverse loads and has a length that is larger than the other two dimensions [14]. There are different beam formulations that can be used to predict its dynamic response. Equation 1 shows the governing equation of a uniform beam undergoing free vibration according to Timoshenko's beam theory [15]. Timoshenko theory accounts for both the bending and shear deflections. If only the first two terms of the PDE are considered, the PDE predicts the beam behavior according to Euler-Bernoulli's theory (which ignores shearing and rotary inertia) [15]. If only the first three terms are considered, the PDE predicts the behavior according to Rayleigh's theory (which ignores shear deflection) [15].

$$EI\frac{\partial^4 u}{\partial x^4}+\rho A\frac{\partial^2 u}{\partial t^2}-\rho I\frac{\partial^4 u}{\partial x^2\partial t^2}-\frac{E}{\kappa G}\frac{\partial^4 u}{\partial x^2\partial t^2}+\frac{\rho^2 I}{\kappa G}\frac{\partial^4 u}{\partial t^4}=0 \quad (1)$$

Where $u(x,t), E, I, \rho, A, G, \kappa, x$ & t are the deflection, tensile elastic modulus, second moment of area cross sectional area, density, shear elastic modulus, shear shape factor, position coordinate and time coordinate respectively [15].

1D FE formulations have been developed for the three beam formulations in the literature [14]–[16]. One of the approaches of deriving the FE formulation, involves reducing the dimension of the PDE using separation of variables knowing that it is an eigenvalue problem and that the time function has a harmonic form [14]. The reduced PDE can be then transformed to the integral weak form by adding a test function and using integration by parts [14]. Afterwards, appropriate shape functions (that satisfy elements boundary condition and interpolation requirements) can be used to determine the element-wise mass and stiffness matrices [14], [15].

The 1D FE code developed in this investigation is constructed on MATLAB® (MathWorks). It first discretizes the domain according to the required number of elements and computes the element-wise stiffness and mass matrices (according to the elements geometric, elastic and mass properties). It then computes the global mass and stiffness matrices according to their nodal connectivity then applies the boundary conditions where appropriate and finally computes the eigenvalues and eigenmodes. The mode shapes are normalized and plotted over the undeformed configuration.

B. Modal Analysis of a simply supported uniform beam.

To validate the developed 1D FE code, the code is tested against an abstract case of a simply supported uniform cylindric beam with the same length to diameter ratio as a TFA system (*L/D*=14.29 where *L* is the combined length of the shortest possible adapter-stem assembly and *D* is the diameter of the intramedullary portion of the stem) where

analytical solutions exist for three beam formulations. Equation 2 shows an example of these analytical solutions for a Timoshenko beam [15].

$$\omega_n^4\left(\frac{\rho r^2}{\kappa G}\right)-\omega_n^2\left(1+\frac{n^2\pi^2r^2}{l^2}+\frac{n^2\pi^2r^2}{l^2}\frac{E}{\kappa G}\right)+\frac{\alpha^2n^4\pi^4}{l^4}=0 \quad (2)$$

Where ω_n is the n^{th} mode frequency, $\alpha^2=\frac{EI}{\rho A}$ and $r^2=\frac{I}{A}$ respectively [15].

Additionally, a 3D ABAQUS® model of the uniform beam is developed. The 3D model treats the beam as a linear isotropic structure made from titanium and uses first order full integration hexahedral elements (C3D8) for the mesh. The 3D model extracts the eigenvalues and eigenmodes using the Lanczos algorithm. This model allows for estimating the out of plane effects and is used to determine if the 1D model has enough approximation power to model the more accurate (3D) implant geometry. Both the 1D and 3D models underwent h-refinement, and the convergence criteria was set to changes of less than 2% for the first five natural frequencies upon at least doubling the number of elements. All the results presented in the next section are for the refined mesh.

C. *Modal Analysis of a simply supported TFA system.*

After validating the code using a uniform beam, modal analysis of a simply supported TFA system composed of an adapter (protruding part of the system) and the stem is performed using the 1D FE code and 3D ABAQUS® models. It should be noted that both models ignore the slight curvature and porous layer of the stem, however the rest of the dimensions were based on measurements of the physical OPL systems. The 1D FE code relied on discretizing the domain into 7 geometric regions as shown in Figure 1. The 3D solid geometry of the adapter and the stem are generated on Solidworks® (Dassault Systèmes). Physically, the stem and the adapter are connected by a threaded screw, however, to simplify the analysis the two surfaces were tied (where the nodes are inhibited from experiencing relative motion) at the interacting region.

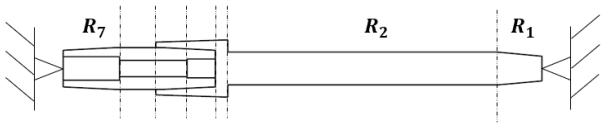

Figure 1. Implant Adapter geometry divided into 7 regions

D. *Modal Analysis of an Osseointegrated TFA system.*

The BII condition is dependent on several factors such as the bone-implant contact area, the material and mass properties of the interface, and the surrounding bone [4]. Previous in-vitro and FE models simplify the interface as a thin uniform layer (0.5-1 mm) with a variable elastic modulus to simulate different healing stages [9], [17]. While this is an oversimplification of the interface condition, it is a reasonable way to control the BII quality in the model using a single parameter. In the current 3D FE model, the interface is simulated using a 0.5 (mm) thick cylindrical layer that is tied from the inside to the stem and from the outside to a thicker cylinder that simulates cortical bone (Figure 2). The material properties of the different components of the model are summarized in Table 1. The cortical bone is fully fixed from the outer side, since it is expected that the amplitude of vibration of the stem-BII region is much more significant than the vibration of the bone which is surrounded by tissues and muscles. This assumption on the boundary condition allows for only modelling the cortical femoral canal region and excluding the femoral head from the model.

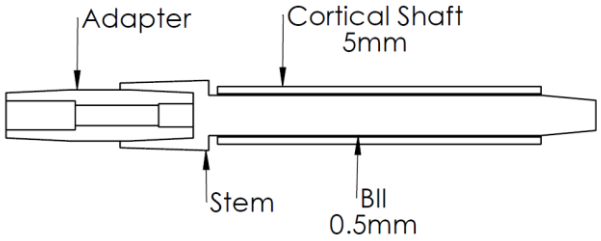

Figure 2. Schematic of the bone-implant system.

Table 1. Material Properties for the different components of the system [18], [19]

Component	Material	Elastic Modulus (MPa)	Poisson Ratio	Density (kg/m^3)
Adapter	Titanium	105,000	0.31	4400
BII	Bone	0.5/9600	0.36	1900
Bone	Bone	16,000	0.36	1900
Stem	Titanium	105,000	0.31	4400

The interface is introduced to the 1D FE model as a set of linear (translational) springs equally distributed at the nodes of R_2 which is the implant's effective length. The spring stiffness is calculated by integrating the stiffness per unit area (k) with respect to the cross-sectional area and length over R_2 and then divided by the total number of springs (Equation 3). Therefore, k can be viewed as a stability metric that is independent of geometric properties R_2. The matching between the 1D and 3D FE model is first performed for an implant with a short stem (effective length=115 mm) by varying the k until the 1st mode matches and then the natural frequency and mode shapes of the remaining modes are compared to the FE model for two extreme interface conditions (E=0.5 and 9600 MPa). The same k that was determined for the shorter stem is used for computing the frequencies and mode shapes for the two extreme interface conditions for a longer implant (effective length = 160 mm) and compared with the 3D FE model. This allows one to check if k has the potential to act as a stability metric that is independent of the geometry.

$$k_s=\frac{2}{N}\int_0^L\int_{-\pi/2}^{\pi/2}kCos(\theta)Rd\theta dL=\frac{4kRL}{N} \quad (3)$$

Where $k_s, N, k, \theta, R \,\&\, l$ are the spring stiffness, number of springs, stiffness per unit area, radial position coordinate, radius and length of R_2 respectively.

III. Results and Discussion

A. Modal Analysis of a simply supported uniform beam.

The natural frequencies of a simply supported uniform beam using different beam formulations are summarized in Figure 3. The reported results are for a mesh of 24 elements (1D model), which satisfied the convergence criteria. As it can be observed, the 1D FE code reaches the analytical prediction for the three beam formulations. This indicates that the 1D FE code is working properly since the mass and stiffness matrices are derived from the governing PDE of each beam formulation and as the number of elements increases, the FE model's approximation power increases and converges to the theoretical solution [15]. Additionally, comparing the three formulations to the 3D ABAQUS model, shows that the three 1D beam models can estimate the first three modes accurately (difference < 5%). However, from the fourth mode onwards more prominent differences between the 3D ABAQUS model and Euler-Bernoulli and Rayleigh theories start to emerge. Euler-Bernoulli and Rayleigh theories overpredict the fifth mode by 13.1% and 9.1% respectively (compared to the 3D ABAQUS® model) while the Timoshenko model is only different by 1.4% from the 3D model. This behavior is expected since Euler-Bernoulli theorem ignores both shear deformation and rotary inertia and Rayleigh's theorem ignores shear deformation [15] and both effects are prominent for the higher order modes. Therefore, the Timoshenko formulation is adopted for the remaining results of the investigation.

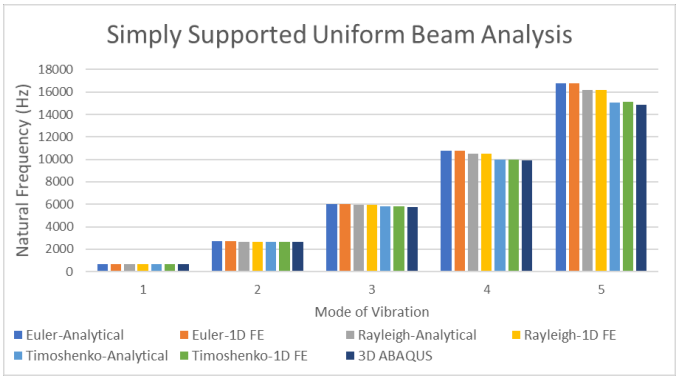

Figure 3. Natural Frequency of a simply supported beam using the three FE beam models, analytical solutions, and 3D ABAQUS® model.

B. Modal analysis of a simply supported TFA implant system.

The first five modes of a simply supported TFA implant system (excluding the BII and the bone) using the 1D FE code and the 3D ABAQUS model are summarized in Table 2. The 1D FE model accurately predicts the dynamic behavior of the stem-adapter, despite its complex geometry, supporting the hypothesis that using an appropriate 1D beam formulation can be used to model the dynamic behavior of the OPL implant systems.

Table 2. Natural Frequency of a Simply Supported TFA system.

	1D FE Model	3D ABAQUS Model	Difference
Mode	$f_n(Hz)$	$f_n(Hz)$	%
1	622.8	620.51	0.37%
2	2711.4	2646.6	2.45%
3	6133.2	6030	1.71%
4	9825.6	9638.1	1.95%
5	15163	14710	3.08%

C. Modal analysis of an Osseointegrated TFA implant.

The 3D ABAQUS model was first used to extract the natural frequency and mode shapes of the first five bending modes, or up until exceeding the 24 (KHz) measurement threshold by one mode, for the short stem for two extreme interface conditions of E=0.5 (MPa) and E=9600 (MPa) which are denoted as LOW and HIGH respectively. The value of interface stiffness in the 1D model (k) was iteratively changed until the first mode matched the 3D ABAQUS® model within ±0.2%. The k values were found to be k=8.2×10^{10} (N/m^3) and 5.5×10^{14} (N/m^3) for the LOW and HIGH BII conditions respectively. Figure 4 summarizes the LOW and HIGH interface cases for the short stem using the 1D and 3D FE models. Using the k found based on the first mode of vibration yields highly accurate results for the LOW interface situation. The results (except for the third mode) are also accurate for the high interface situation. In terms of the mode shapes, the 1D FE model captured highly similar deformation patterns (mode shapes) for all the modes of vibration. Figure 5 and Figure 6 are selected excerpts of the first and fourth mode of vibration (the BII and bone were suppressed for visualization) for the LOW stiffness case. Even the relatively complex bending behavior of the fourth mode was captured appropriately using the 1D model. The third mode of the HIGH stiffness had the highest difference of 9.2% is shown in Figure 7. The 3D ABAQUS® model reveals that the behavior for this mode is not strictly bending (with significant axial and out of plane effects) and this is a plausible explanation for the higher difference between the 1D and 3D models. However, the initial conditions are not expected to trigger this mode, since the loading is transverse and so the effect of this mode is not expected to be significant on the time domain response. Additionally, this mode is mostly contained within R_1 where the BII does not develop and is believed to have little effect on the structural stability of the OPL bone-implant system [20].

This work was supported by the Department of Defense, FY20 Peer Reviewed Orthopaedic Research Program (W81XWH-21-1-0857), Glenrose Rehabilitation Research Innovation and Technology (GRRIT), Mathematics of Information Technology and Complex Systems (Mitacs IT15524) and the Natural Sciences and Engineering Research Council of Canada (NSERC).

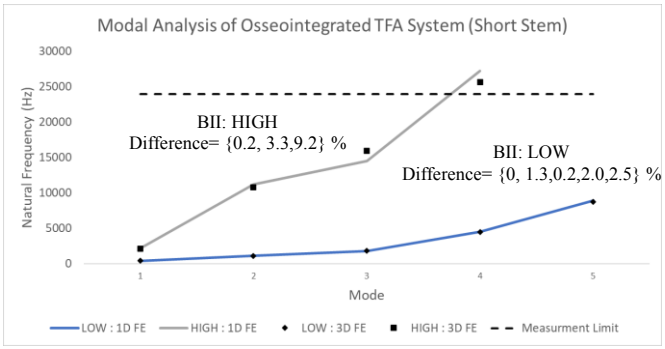

Figure 4. Natural Frequencies of the short TFA stem for LOW (E=0.5 MPa & k=8.2×10¹⁰ N/m³) and HIGH BII conditions (E=9600 MPa & k=5.5×10¹⁴ N/m³)

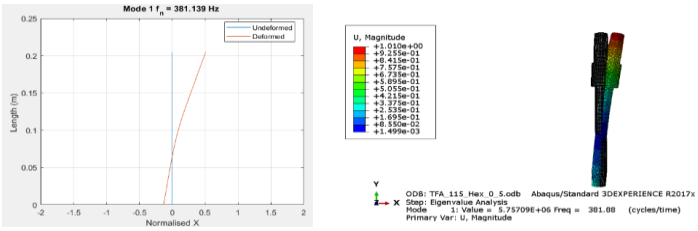

Figure 5. First mode of a short stem for LOW (E=0.5 MPa & k=8.2×10¹⁰ N/m³) condition using the 1D (left) and 3D (right) FE models

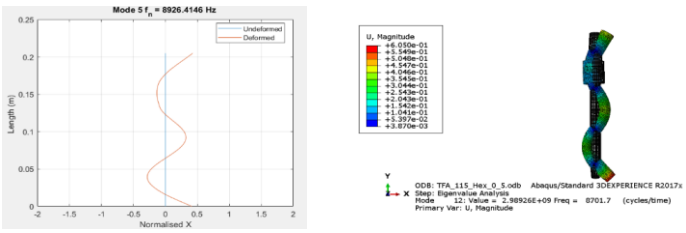

Figure 6. Fourth mode of a short stem for LOW (E=0.5 MPa & k=8.2×10¹⁰ N/m³) BII condition using the 1D (left) and 3D (right) FE models

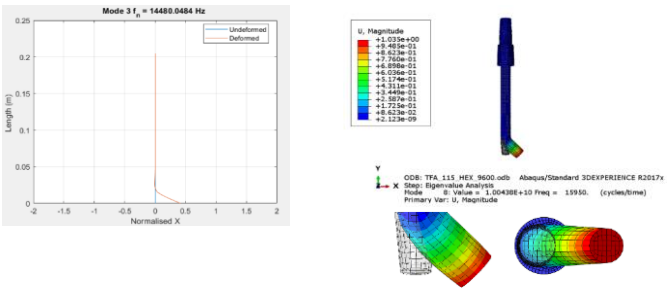

Figure 7. Third mode of a short stem for HIGH (E=9600 MPa & k=5.5 ×10¹⁴ N/m³) BII condition using the 1D (left) and 3D (right) FE models

Using the same values of *k* found for the short stem, the 1D FE model was used to extract the natural frequencies and mode shapes for the long stem and the results were compared to the 3D ABAQUS® model. The results are shown in Figure 8 for both interface conditions. There is excellent agreement between the 1D and 3D FE models with an average and maximum difference of 1.3% and 2.5% respectively for the LOW interface condition. While the higher BII condition had an average and maximum difference of 3.9% and 7.6% (excluding the fourth mode as it exceeds 24 (KHz)) respectively.

The results presented here indicate that the *k* can be used as an absolute metric to compare between implants of different geometries since the same *k* of the short stem genereated a similar dynamic response between the 1D and 3D ABAQUS® models for the long stem for the same values of *E*. The sensitivity of the natural frequency to the implant geometry has been a major limitation to implant stabillity assessment using vibration methods [12], [21]. It has been proposed that using torsional modes of vibration can be more sensitive to the interface conditions and less dependent on the system's goemetry for dental implants [22], however torsional modes can subject the implant to danegrous loads and lead to loosening. Mathematical modelling of hearing aids and natural teeth using the ASIST to estimate the stiffness of the BII directly has demonstrated that this approach increases the sensitivity towards the BII and is less sensitive to the system's geometry compared to the natural frequency without subjecting the bone-implant system to torsional modes [7], [8], [13].

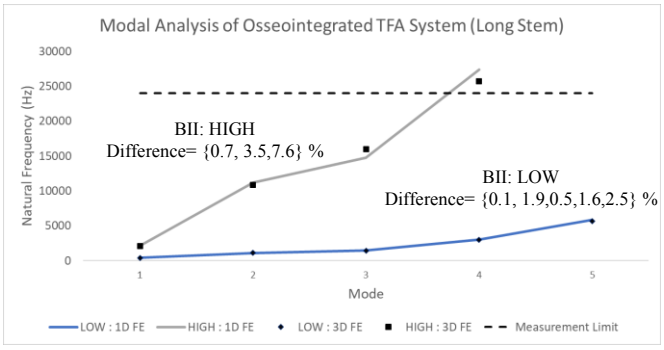

Figure 8. Natural Frequencies of the long TFA stem for LOW (E=0.5 MPa & k=8.2×10¹⁰ N/m³) and HIGH BII conditions (E=9600 MPa & k=5.5×10¹⁴ N/m³)

IV. CONCLUSION

In this investigation, a 1D FE model of the OPL TFA bone-implant system was developed based on Timoshenko's beam formulation. Modal analysis of a simply supported uniform beam (same *L/D* ratio of a TFA implant configuration) showed that the code's solution converged with the analytical solutions of Euler, Rayleigh, and Timoshenko theories. It also showed that Timoshenko is the most appropriate formulation since shearing effects can be significant for the higher order modes. Furthermore, modal analysis of a simply supported 1D TFA implant system showed that the 1D model captured the bending modes of interest accurately with a maximum difference of 3.08% when compared to a 3D ABAQUS model®. Finally, the BII was introduced to the 1D model as a series of linear springs distributed over the stem's effective length. The analysis was first carried out for a short stem (effective length of 115 (mm)) and the *k*, in (N/m^3), of the BII was found by matching the first

mode frequency with the 3D Model for two extreme interface conditions. The natural frequencies and mode shapes of the remaining modes were highly similar to the 3D model. The same values of k found for the short stem, were used to compute the natural frequency and mode shapes for a long stem (effective length of 160 mm) and they matched the 3D FE model. This indicates that the k was not influenced by the stem's length and has the potential to be an absolute stability metric.

Accurate prediction of the natural frequencies and mode shapes sets the foundation for the accurate prediction of the time domain response of the system. The numerical analysis laid out in this work thus formulates the basis for a series of additional mathematical, in-vitro and in-vivo analysis of osseointegrated TFA implant systems and the development of a stability measurement system. Future work would involve: (1) using the 1D model to evaluate the time domain response of the system, (2) validating the response experimentally (in-vitro and in-vivo) and to a 3D FE time integration model, (3) replacing the tied interaction with springs that can model screws, (4) optimizing the measurement and loading protocols and (5) performing parametric studies on the effect of the material, surface properties and distribution of the BII on the response.

ACKNOWLEDGMENT

The authors would like to thank and acknowledge Professor Gary Faulkner for his work and support on this study. This work was supported by the Office of the Assistant Secretary of Defense for Health Affairs through the FY20 Peer Reviewed Orthopaedic Research Program, endorsed by the Department of Defense under Award No. W81XWH-21-1-0857. Opinions, interpretations, conclusions and recommendations are those of the author and are not necessarily endorsed by the Department of Defense.

REFERENCES

[1] K. Hagberg and R. Brånemark, "One hundred patients treated with osseointegrated transfemoral amputation prostheses - Rehabilitation perspective," *J. Rehabil. Res. Dev.*, vol. 46, no. 3, pp. 331–344, 2009.

[2] M. Al Muderis, W. Lu, K. Tetsworth, B. Bosley, and J. J. Li, "Single-stage osseointegrated reconstruction and rehabilitation of lower limb amputees: The Osseointegration Group of Australia Accelerated Protocol-2 (OGAAP-2) for a prospective cohort study," *BMJ Open*, vol. 7, no. 3, pp. 1–4, 2017.

[3] J. S. Hoellwarth, K. Tetsworth, S. R. Rozbruch, M. B. Handal, A. Coughlan, and M. Al Muderis, "Osseointegration for Amputees," *JBJS Rev.*, vol. 8, no. 3, pp. 1–10, 2020.

[4] X. Gao, M. Fraulob, and G. Haïat, "Biomechanical behaviours of the bone – implant interface : a review," *J.R.Soc.Interface*, vol. 16, pp. 1–20, 2019.

[5] E. M. Zanetti, G. Pascoletti, M. Cali, C. Bignardi, and G. Franceschini, "Clinical Assessment of Dental Implant Stability During Follow-Up : What Is Actually Measured , and Perspectives," *Biosensors*, vol. 8, no. 68, pp. 1–18, 2018.

[6] L. Sennerby and N. Meredith, "Implant stability measurements using resonance frequency analysis: Biological and biomechanical aspects and clinical implications," *Periodontol. 2000*, vol. 47, no. 1, pp. 51–66, 2008.

[7] L. Westover, G. Faulkner, W. Hodgetts, and D. Raboud, "Comparison of implant stability measurement devices for bone-anchored hearing aid systems," *J. Prosthet. Dent.*, vol. 119, no. 1, pp. 178–184, 2018.

[8] M. Mohamed, H. Pisavadia, and L. Westover, "A finite element model for evaluating the effectiveness of the Advanced System for Implant Stability Testing (ASIST)," *J. Biomech.*, vol. 124, 2021.

[9] F. Shao, W. Xu, A. Crocombe, and D. Ewins, "Natural frequency analysis of osseointegration for trans-femoral implant," *Ann. Biomed. Eng.*, vol. 35, no. 5, pp. 817–824, 2007.

[10] N. J. Cairns, M. J. Pearcy, J. Smeathers, and C. J. Adam, "Ability of modal analysis to detect osseointegration of implants in transfemoral amputees: A physical model study," *Med. Biol. Eng. Comput.*, vol. 51, no. 1–2, pp. 39–47, 2013.

[11] N. J. Cairns, M. J. Pearcy, J. Smeathers, and C. J. Adam, "Simulating the bone-titanium interfacial changes around transfemoral osseointegrated implants using physical models and modal analysis," in *1st International Workshop on Innovative Simulation for Health Care, IWISH 2012, Held at the International Multidisciplinary Modeling and Simulation Multiconference, I3M 2012*, 2012, pp. 1–9.

[12] V. Pattijn, C. Van Lierde, G. Van Der Perre, I. Naert, and J. Vander Sloten, "The resonance frequencies and mode shapes of dental implants: Rigid body behaviour versus bending behaviour. A numerical approach," *J. Biomech.*, vol. 39, no. 5, pp. 939–947, 2006.

[13] L. Westover, G. Faulkner, W. Hodgetts, and D. Raboud, "Advanced System for Implant Stability Testing (ASIST)," *J. Biomech.*, vol. 49, pp. 3651–3659, 2016.

[14] J. N. Reddy, *Introduction to the Finite Element Method*, 4th Editio. McGraw Hill, 2019.

[15] S. S.Rao, *Vibration of Continous Systems*, Second Edi. New Jersey: Wiley, 2019.

[16] B. S. Gan, *An Isogeometric Approach to Beam Structures*. Springer, 2018.

[17] S. Lu, B. S. Vien, M. Russ, M. Fitzgerald, and W. K. Chiu, "Quantitative monitoring of osseointegrated implant stability using vibration analysis," *Mater. Res. Proc.*, vol. 18, pp. 87–94, 2021.

[18] Engineering Toolbox, "Metals and Alloys-Densities," 2004. [Online]. Available: https://www.engineeringtoolbox.com/metal-alloys-densities-d_50.html.

[19] SAWBONES, "Biomechanical Materials for Precise, Repeatable Testing." [Online]. Available: https://www.sawbones.com/biomechanical-product-info. [Accessed: 21-Jan-2022].

[20] S. Thomson, A. Thomson, K. Tetsworth, W. Lu, H. Zreiqat, and M. Al Muderis, "Radiographic Evaluation of Bone Remodeling Around Osseointegration Implants Among Transfemoral Amputees," *J. Orthop Trauma*, vol. 33, no. 8, pp. 303–308, 2019.

[21] E. M. Zanetti *et al.*, "Modal analysis for implant stability assessment : Sensitivity of this methodology for different implant designs," *Dent. Mater.*, vol. 34, no. 8, pp. 1235–1245, 2018.

[22] M. Zhai, B. Li, and D. Li, "Effects on the torsional vibration behavior in the investigation of dental implant osseointegration using resonance frequency analysis : a numerical approach," *Med. Biol. Eng. Comput.*, vol. 55, no. 9, pp. 1649–1658, 2017.